Characterization and Performance Analysis of UHF RFID Tag for Environmental Sensing Applications

by

Zhen Zhong Li

A thesis
presented to the University of Waterloo
in fulfillment of the
thesis requirement for the degree of
Master of Applied Science
in
Electrical and Computer Engineering

Waterloo, Ontario, Canada, 2012

Author's Declaration

I hereby declare that I am the sole author of this thesis. This is a true copy of the thesis, including any required final revisions, as accepted by my examiners.

I understand that my thesis may be made electronically available to the public.

Abstract

Passive radio frequency identification (RFID) tag has been shown efficient in item tracking and management in the supply chain. Attracted to low weight and small size of wireless nodes, some research work was conducted to extend the RFID advantage into environmental sensing applications. The concept is to using tag frequencies as sensing parameters. When variation occurs in the surrounding environment, such as temperature and humidity level, the operation frequencies of tags would be shifted, and such shift can be used to identify the degree of variation in the environment. One challenge of RFID tag is the distortion from other surrounding objects, the existence of obstacles and metals can have greatly impact on the sensing performance in both accuracy and sensing range.

This thesis work conducts an investigation of the performance of a passive radio-frequency identification (RFID) based system. The investigation systematically probed the effects of passive RFID tag orientation and obstacles (blocking line-of-sight between a reader and a tag) as well as reading period (the time required for successful detection) on the range of detection. In the absence of obstacles, optimized tag orientation improved the system reliability and range of detection. At a reading distance where tag readability became unstable, increasing the reading period led to a higher reliability. A theoretical model was also established and was in good agreement with measurement results, providing a simple guideline to the further experiments.

This work would also advance the knowledge understanding on wireless sensing on metal effect, humidity and temperature.

Acknowledgements

I would like to first express my sincere gratitude to my advisors, Professor Dayan Ban for all of the supervision, patience and time dedicated throughout my research work and in writing of this thesis. The encouragement and willing to share all of the ideas and experiences was crucial to my progress.

I would like to also express my great appreciation to Dr. Nezih Mrad and Dr. George Xiao for their guidance and support at Nation Research Council of Canada and Defence Research and Development of Canada. Their knowledge and skill in the research field are invaluable in accomplishing this thesis. It was a great experience working under their supervision.

I would like to thank Professor Cui for reviewing this thesis and his valuable comments.

It was my pleasure to work with my friendly colleagues and friends, and thanks for their supports and discussion on both academic and non-academic matters. Also, I like to give thanks to the Nation Research Council of Canada, Defence Research and Development of Canada, University of Waterloo and the ECE department for supporting my research.

Lastly, I am thanking my parents and family for their devotion on me through the years.

Dedication

To my parents for their great effort and unconditional support…

There is no doubt in my mind that without their continued support and counsel in my life I could not have completed this process. All the care and advices are the lamp unto my feet and a light unto my path and resided deeply in my heart and memory. It is my honor to have you as my parents and my fortune to be your son.

Thank you!

Contents

List of Figures

List of Tables

List of Abbreviations and Acronyms

CIM	Chemically Interactive Material
CNT	Carbon naotube
DOD	Department of Defence
GIS	Geographic Information System
GPS	Global Positioning System
HF	High Frequency
IDT	Inter-digital Transducer
QMB	Quartz Micro Balances
RF	Radio Frequency
RFID	Radio Frequency Identification
SAW	Surface Acoustic Wave
TSM	Thickness Shear Mode
UHF	Ultra High Frequency
UPC	Universal Product Code

Chapter 1

Introduction

Sensor technologies have long existed in the scientific field for the purpose of monitoring subjects, and environmental sensors are the ones typically monitoring the state of their surrounding environment, such as in-door air quality, temperature, humidity, carbon dioxide level and many others. The environment sensor network extends mankind's abilities on environmental control to prevent undesired occurrence and tragedies. One typical example in practical use of sensing technology is smoking detectors in residential houses. The applications of environment sensors are widely spread out in many fields, including structure monitoring for buildings and constructions, health monitoring for patients' conditions, and item tracking for inventory management.

The trend of sensor technologies is moving towards wireless, and wireless technology has seen significant development over the past decade. Compared to a wired sensor network, a wireless sensor network is more flexible in general. Adding a wireless sensor node to the network is much more convenient without the concern on the path of wiring and the length of wire. For example, in health monitoring for patients' conditions, a wired device would require patients to stay close to the monitoring device. Less weight and smaller size are the other advantages of wireless sensors. In the applications where space is sensitive and crucial, such as structural health monitoring on aircrafts in aerospace application, the space of an aircraft is limited and weight is expected to be as low as possible.

1.1 RFID Technology

A basic passive RFID system, as shown in Figure 1(a), is consisted of three components: a host (including a database) for information management and control, RFID tags which contain the information of items that they attach to, readers to retrieve information from the tags and transmit the information to the host where the data is stored and processed.

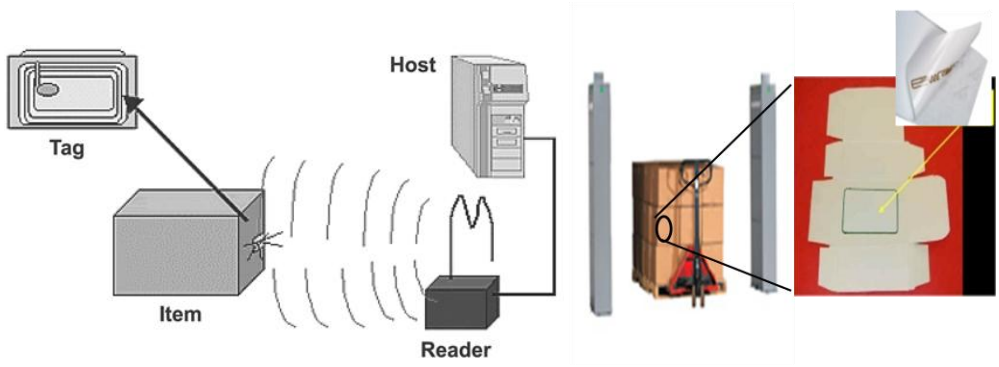

(a) (b)

Figure 1: RFID Tracking System; (a) a basic RFID system and its component [1]; (b) warehouse implement demonstration [2].

RFID tags serve the same purpose as a bar code or a magnetic strip on the back of a credit card or ATM card, to track, store and provide unique identification of the objects [3]. However, RFID technology can address problems that other technology cannot. People have to scan the bar code manually each time to track the item when it moves; Ultrasound and infrared technologies cannot penetrate materials, so it would require an open box examination to trace what is inside; GPS, on the other hand, does not work well in an indoor environment [4].

Beside passive tags, there are also other types of RFID tags. Generally speaking, the RFID tags are usually categorized as passive tags, active tags and semi-passive (or semi-active) tags based on whether the tags have their own power source, such as batteries. The general pros and cons of the RFID technology are discussed as following.

Some of the typical advantages of RFID technology are [5]:

- Robust tags that can stand extreme conditions and temperatures;
- Tags are available in a great range of types, sizes and materials;
- No need for physical contact between the data carrier and the communication device.
- The Tags can be used repeatedly;
- Relatively low manufacture and maintenance cost;
- An RFID tag could identify the item and store detailed information about the item;

Benefits of RFID applications are [6]:

- Total asset visibility;
- Tracking for incoming and outgoing deliveries;
- Full inventory history and records;
- Localization of items;
- Real-time security;

Common Problems with RFID:

- Reader Collision – occurs in RFID systems when the coverage area of one RFID reader overlaps with that of another reader, due to signal interference or multiple readers of the same tag [7].
- Tag collision – occurs when multiple tags are energized by the RFID tag reader simultaneously, and reflect their respective signals back to the reader at the same time [8].

Other potential issues and concerns about RFID:

- Security and privacy issue – due to limited resources that can be dedicated to security functions [9];
- Health concern – due to long period exposure to the RF electromagnetic fields. However, there are no evidences showing that there is a health risk [10].

1.2 Problem Description and Motivation

RFID technology has been proven to be successful in item tracking. Tags contain unique identifications enable asset tracking ability. To extend the ability of RFID, it is always the interest to provide more information on the tracked asset, not only tracking the location but also monitoring the state.

In the field of aerospace, temperature and humidity are the initiators and promoters for corrosion and crack on air-vehicles. They are looking for wireless solutions of detecting and monitoring cracks and their development. Although wired solutions are available, they no longer meet the needs of nowadays aircraft. Space and weight become critical to most air vehicles. When aircraft is getting more and more sophisticated, wired sensors gradually become an issue, since such aircraft may employ hundreds of wired sensors for state monitoring which results tons of wire in weight. To more effectively and efficiently operate aircraft, wireless solution becomes curial to reduce the weight and to improve space efficiency.

Passive ultra high frequency (UHF) RFID tag which is designed with the feature of small size and no power consumption satisfies the demand on wireless solution for air vehicles. An UHF RFID based sensor would be suitable for essential requirements. The concept is to use the UHF RFID tag as a sensing platform. On this platform, a sensitive layer is deposited. By monitoring the frequency displacement of the tag caused by the sensitive material reacted to humidity and temperature, the degree of the change can be determined.
Significant efforts have been devoted to develop sensors using RFID tag as the wireless node for communication, such as RFID based surface acoustic wave (SAW) sensors and carbon nano-tube (CNT) sensors, which is described in more detail in chapter 3. More recently, some scientists start to implement RFID tags for sensing applications. It has been reported to use high frequency (HF) RFID tags for chemical sensor applications. Nevertheless, UHF tags which are commonly used for logistic and item tracking, have not seen much progress in chemical sensing application. The main obstacles are noted following:

RF signal absorption – It is a known issue that when a UHF tag is directly attached to metal surface, it would lose its function (both forwards and backward communication). The current solution, or so call “metal” tag, contains a cover on the original tag to create a displacement between the tag and the metal surface.

Path loss formulation – Path loss is always a challenge in the signal transmission. The present of objectives in the surrounding environment would simply increase the difficulty of the formulation. Although there are many research works on path loss formulation, there is not a universal solution or method for it.

Signal interference – As a result of multipath generated from reflection and deflection, signal overlapping and collision results noise in measurement accuracy.

1.3 Sensing Platform and Approach

The concept of this approach is using RFID tag as a sensing platform. Shown in Figure 2, a sensing film is layered at the top of the tag. The sensing film is directly deposited on the tag antenna. Such deposition would modify the characteristic of the original tag by changing its impedance, which, in turn, modifies the operation frequency of the tag. The new operation frequency and corresponding characteristics are used as the sensing baseline to sense targeted analytes as shown in Figure 3. The added layer can be treated as a simplified R-C circuit with a resistant value of R and a capacitor value of C, in addition to the circuit of the tag itself.

When an analyte presents, the reaction between the analyte and the sensing film would again modify the impedance of the tag. Now the sensing circuit is presented by the circuit with a resistor R_f and a capacitor of C_f. By comparing the status of the tag after reaction to the baseline and measuring the changes in the sensing parameter, in other words, by comparing the differences between R and R_f and the differences between C and C_f it is possible to determine the type of the analyte.

This approach was first described by Radislav Potyrailo on a high frequency tag that operates at 13.56MHz and operating frequency is the measuring parameter. His experiment demonstrated a possibility of detecting different types of chemicals, which is detailed in Chapter 3. We would like to apply the similar principle on the ultra high frequency tags for chemical and corrosion detections. Our first step is to evaluate the impact of the deposition on the tag itself before any reaction is taken in place as shown in Figure 3(a), and it is one major objective of this thesis. To select suitable sensing films and corresponding analytes, a literature review is also conducted and presented in the next chapter.

1.4 Thesis Contribution

The major contribution of this thesis is to propose a model to evaluate the performance of a RFID system and validate the feasibility of the model based on the system performance toward wireless sensor. To this end, the research objectives are defined as:

- To evaluate the effect of sensing distance and path loss in the present of obstacle on the performance of the RFID system.

- To formulate a model to simulate and simplify the evaluation procedure of the environmental effect. The model would take into account of the effects of distance and both ideal (free space) and non-ideal conditions and predict the performance in specific conditions when tag is attached to wood, metal and other materials.

- To explore the effects of humidity and temperature on the characteristics of the RFID system. The impact of surrounding environment condition on the RFID system must demonstrate the sensitivity and possibility towards a temperature or humidity sensor and to a long term goal as a corrosion sensor.

The empirical experiment results are reported and discussed to demonstrate the evaluation process in practical use.

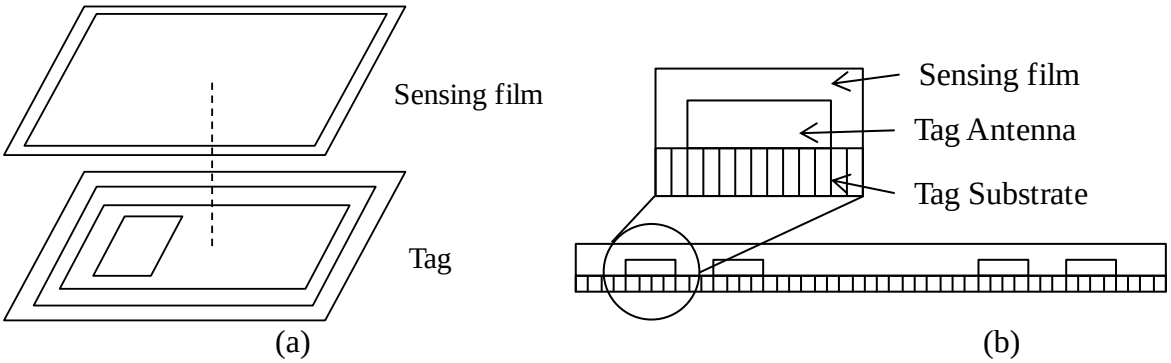

Figure 2: Schematic diagram of RFID sensing platform; (a) sensing layers; (b) sensing film deposition.

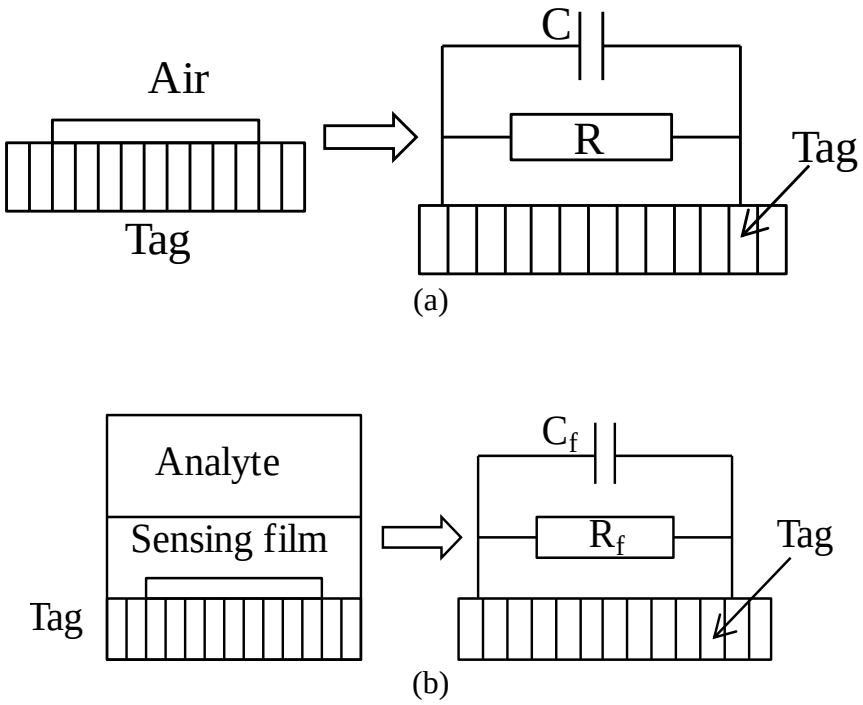

Figure 3: modeling presentation of sensing process; (a) tag exposed to air; (b) tag coated with sensing film and then exposed to analyte.

1.5 Thesis Organization

The reminder of this thesis is organized as follows:

Chapter 2 describes the overview of RFID system and background of relevant materials. It first introduces the current state of RFID system and its marketing potential, followed types of RFID system as well as detail concept on our approach.

Chapter 3 presents the literature work of related to wireless sensor development and work towards RFID sensors. The literature work mainly focus on surface acoustic wave (SAW) and carbon nano-tube (CNT) sensors and their work towards RFID technology.

Chapter 4 provides the theoretical development and simulation proposed for the evaluation of a RFID system. It highlights the model prediction on the behavior of radio frequency signal in an open environment. This includes near field effect and far field effect and classifies the region of the behavior changes.

Chapter 5 and 6 reports our experimental results from our evaluation process. Chapter 5 reports on sensing distance, obstacle and orientation effect on the performance of RFID system, while chapter 6 reports on humidity and temperature effect. The set of experiments is targeted to evaluate the feasibility and reliability of the system as well as to validate the theoretical modeling.

Chapter 7 concludes the research work. It highlights research contribution and provides recommendation on future work related research work.

Chapter 2

Overview of RFID Technology

This chapter provides the background information of the RFID technology. Section 2.1 presents the current state of RFID technology and its market value. Section 2.2 compares two major technologies, barcode and RFID in the field of logistics. Section 2.3 and 2.4 details the types and concept of RFID technology. Section 2.5 suggests the choice of antenna and section 2.6 provides information on the RFID tag inlay.

2.1 Current Market of the RFID Technology

The growth and development of wireless technologies on sensing have attracted many attentions and the growing interests on the wireless technologies create a large market for investments.

One report [12] by Kevin Gainer in 2009 on the market of environmental sensors indicated that the global market for environmental sensing and monitoring technologies was worth $9.1 billion in 2008 and estimated a value of $10.1 billion for 2009. This was expected to reach $13 billion in 2014. This report covers the sensor industry and its structure, markets and applications of the sensors as well as companies profiles on the sensors. For the remote and wireless sensing technology, Jim Wilson reported [11] in 2007 that the total global market expenditures for remote sensing products were more than $7 billion in 2006 and expected to reach almost $7.3 billion in 2007. By 2012 the market would reach more than $9.9 billion. This report further detailed an overview of the remote sensing industry, including descriptions of global positioning system (GPS), Geographic information system (GIS), and applications, including weather forecasting, intelligence gathering, climate change, public health. A market analysis on these applications is also provided.

Besides, wireless technology has seen significant development over the past decade. In the field of logistics, passive Radio Frequency Identification (RFID) technology has shown its capacity on tracking and managing a large amount of items. The enforcement of implementation of the RFID technology in the supply system by organizations such as Department of Defense (DOD) on its military supplements and Wal-Mart on its shipments has brought the technology to eyes of thousands companies worldwide. The success on the focused logistics led by these two organizations and the attractive characteristics of reduced size and weight and no power requirement attract more and more attention to the technology

and result an increase on the adoption of the technology. The global market value for radio frequency identification (RFID) technologies was $6.4 billion in 2010. That value is projected to reach $11.3 billion in 2015 in by the electronics industry market research and knowledge network in its report "RFID: Technology, Applications, and Global Markets" [13].

Ultra high frequency passive tags are most frequently used in the warehouse. These tags are placed on the containers of the items, such as inside the cardboard box as in Figure 1 (b). When the box is passing through a gateway or a check point, the reader at that gateway detects the tag embedded inside container and records the identifications of the sealed objects and then transmits the corresponding information to the remote host for tracking and management. Before RFID is first introduced in warehouses, the most common one is barcode.

2.2 RFID vs. Barcode

In the field of logistic, traditional method of tracking and management of goods is done through barcode, which requires line of sight while scanned. The RFID tag, on the other hand, is more flexible on its position while read and can be even embedded inside the cardboard of the box with insignificant impact on its readability, which increases the security of the tag itself. The automatic reading system can reduce the work and time of scanning process required by the barcode.

(a)

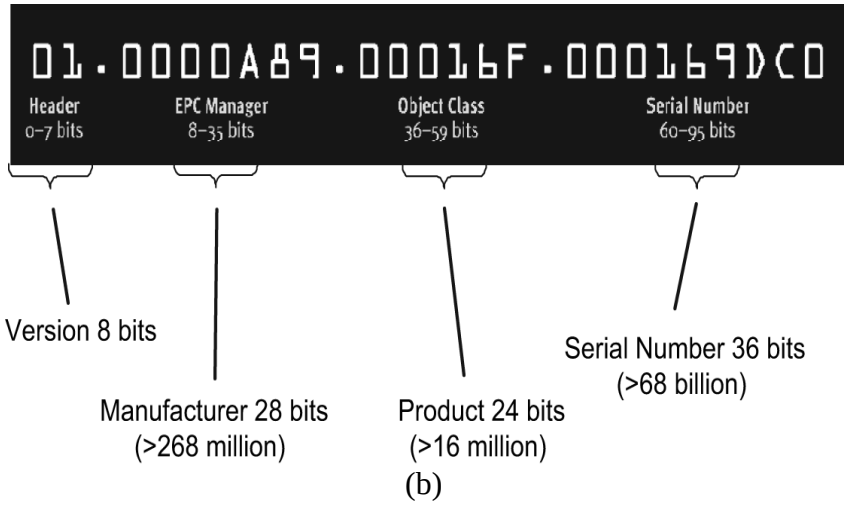

(b)

Figure 4: Barcode and RFID Technology; (a) barcode standard; (b) RFID standard [14].

In addition, the RFID tag is using digital memory for information storage rather than graphic presentation as it is for the barcode. Figure 2 compares the typical standards of the two technologies. For the 12 digit barcode using Universal Product Code (UPC), it has a header digit, 6 digits to indicate manufacturer and 4 digits to identify the type of the item, with one checking digit. It should be noted that barcode only identify the type of the item but does not distinguish the products of the same type. For example, two bottles of milk from the same manufacturer have the identical barcode number. On the other hand, RFID has a 2-digit version number and 28 digits for manufacturers which are 23 digits more than the barcode. It also has a 24 digits of product number which are 20 digits more than the barcode. In addition, it includes a serial number to identify each individual items of same type, which means it is able to identify each bottle of milk even though they are from the manufacturers.

With digital memory, RFID is able to carry massive data and offers more and detailed information of the object. Thus, tracking can be more accurate and precise with RFID system. Besides, digital memory can be rewritable, enabling reuse of the tag and modification of the information, while for barcode, any modification requires a replacement and barcode reaches end of its life cycle when the item is delivered to its destination. The major differences between two logistic technologies are summarized hereby:

Table 1: Comparison of two logistic technologies, Barcode and RFID [15, 16]

Attribute	Barcodes	RFID Tags
Technology Standard	Optical, image technology ISO/IEC 15426-1 (linear) ISO/IEC 15426-2 (2D)	Radio frequency, wireless ISO/IEC 18000(Item Management) ISO/IEC 14443 (Proximity cards) ISO/IEC 15693 (Vicinity cards)
Data capacity	Up to 24 characters for linear presentation and up to 2000 characters for two dimensional barcode	Several thousand characters
Reading requirements	Line of sight required	Within the detection range
Durability	Subject to wear/damage or removed; cannot be read if	Can be hidden but subject to certain environmental impact (by

	dirty or greasy	metal, liquids, etc.)
Security	Data can be easily reproduced	Data can be encrypted and a "kill" feature to remove data permanently
Read Rate	One at a time, slow and slower for two dimensional barcode;	Multiple tags can be read simultaneously
Read and write	Read only	Tags can be both read only and rewritable
Human Capital	Scanned by human in general	Scan process can be automated
Convenience	Barcode can be electronic generated so it can be printed or reproduced at any printer via internet	Tag has to be made at manufacture or requires a sophiscated RFID printer.
Event Triggering	Not possible with barcode	Yes (door opening, alarm, etc.)

Due to the nature optical image technology, barcode is visible, with no protection against information access and reproduction. That exposure reduces its duration and security compared to RFID technology based tag, which can be hidden or sandwiched between layers. Although exposure and easy reproduction scarifies the security level, it increases its convenience. Can be printed on most printers of the world via internet access makes the information easy to transfer. As a result, although passive RFID tags exceed barcode in several categories, RFID is still seen as a complementary to barcode by some viewers because of the convenience. Barcode is much easier to reproduce and can be electronic generated. Thus, the intention now is to store basic identification on barcode and more sensitive information on RFID tag.

2.3 Types of RFID

Readers and tags are two major components of the RFID system. Tags store identification of the object, while readers transmit signals and retrieve it. For different types of tags, readers are designed differently and implemented with different standards. A typical RFID reader contains Transmitter (signal modulation), baseband processor, circulator and receiver (signal demodulation) as well as the reader antenna. Different RFID technologies require different modulation modules. This section will focus on the types of technologies used in RFID system from tag aspects.

There are several ways that RFID tags can be classified depending on the criteria, such as frequencies and protocols. Generally speaking, the RFID tags are usually categorized as passive tags, active tags and semi-passive (or semi-active) tags based on whether the tags have their own power source, such as batteries.

(a) (b) (c)

Figure 5: RFID Tags; (a) passive; (b) semi-passive/active with battery source; (c) active [17, 18].

Passive tag – has no internal power supply. When a RFID reader is approaching, the tag retrieves power from signals emitted by the reader to operate, and then it transmits data to the reader by inductive coupling or backscattering techniques, which are revealed in next Section 2.4. It can be flat and thin as shown in Figure 3(a).

Semi-passive/active tags – have their own power sources but just for powering the chips but not for data transmission. Since no demand on power from the reader, all signal power from the reader is used for data transmission, with a better response and detection range to reader signal compared to passive tag. Both inductive coupling and backscatter coupling technologies are seen in the data transmission for this type of tags. As illustrated in Figure 3(b), the tag contains a button cell type battery for the processor so that all received power can be used for transmitting back the signal which is stronger than passive transducer. This allows increasing communication distance with quit cheap solution [17].

Active tags – requires their own power sources to generate outgoing data signal. Differed from previous two types of tags, active tags can be treated as standard-alone wireless nodes. By having own power supply, active tags usually have better performance than passive tag, having more memory, more power to send outgoing signal far away. Besides, most of active tags can be programmed.

Table 2: Summary of characteristics of different types of tags

Attribute	Passive Tag	Active Tag	Semi-passive/active Tag
Internal Power Source	No	Yes	Yes
Response Distance	Short	Very long	Long
Weight	Light	Less light	Less light
Cost	Cheap	Expensive	Less expensive
Life Cycle	Long	Short	Long

Table 2 summarizes the major differences among the types of the tags. Because of existence of the power source and life cycle of passive tag is generally longer. In addition, with a much complex design, active and semi-passive/active is much expensive compared to passive tag, and that complexity also increase on the weight of the tags. The passive nature with less weight and longer life time proves the passive tag is a better candidate than other two as the platform for chemical sensing.

2.4 Data Transmission Techniques

There three major techniques that are used in data transmission in radio frequency and its applications: capacitive coupling, inductive coupling and backscattering. Each technique has its advantages and disadvantages, which is presented in detail.

2.4.1 Capacitive coupling

Capacitive coupling transfer electromagnetic energy via mutual capacitance rather than mutual inductance. When two circuits are placed close enough the circuits create a mutual capacitance between them, acted as dielectric materials. Smart card is a typical example and where the majority of the application involve. The reading range is generally less than 2 centimeter as defined by ISO standard 10536. A typical frequency is 125kHz.

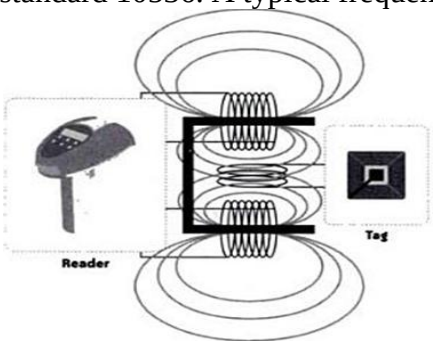

Figure 6: Capacitive coupling; tag is inside into the reader for communication.

As shown in Figure 8 for a smart card reader and a tag from a smart card that is inserted into the reader, capacitance is created at both above and below the tag. The capacitance is measured by the electrical storage capacity and voltage cross them. When a signal is generated in the reader, the signal is transferred through the changes in the across voltage and then used to power up the tag in the same as inductive coupling. The signal is also returned by load changing in the same way as inductive coupling. However, for mutual capacitance to exist, the distance between two circuits are limited, within a few millimeters and less than a few centimeters. Different from inductive coupling, which is based on magnetic field, and whose reading range can be extended by a larger antenna area, the antenna for capacitive coupling is not as they are replaced by electrodes. As the result, the reading range based on capacitive coupling is usually less than other techniques.

2.4.2 Inductive coupling

There are two major types of techniques are used in RFID wireless transmission for contactless communication, inductive coupling and backscattering coupling. Figure 5 describes the inductive coupling principles.

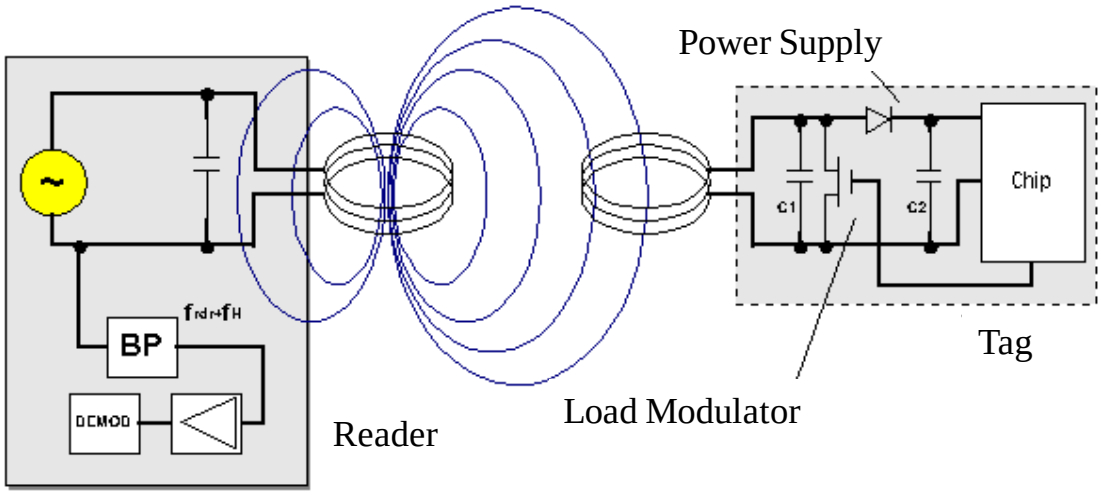

Figure 7: Inductive coupling between the reader and the passive tag [20].

On the reader side, receiver is designed with coupling effect as presented in Figure 5. A part of the emitted field penetrates the antenna coil of the transponder by induction, which generates a voltage in the transponder's antenna coil serving as the power supply for the microchip. To provide such electromagnetic field, a capacitor is carefully selected in parallel with the reader's antenna coil to form a parallel resonant circuit, which introduces a very high current in the antenna coil of the reader by the resonance. As energy is drawn from the reader to the transponder, the additional power consumption can be measured as the voltage drop at the internal resistance in the reader antenna. Here is how data is transferred from transponder.

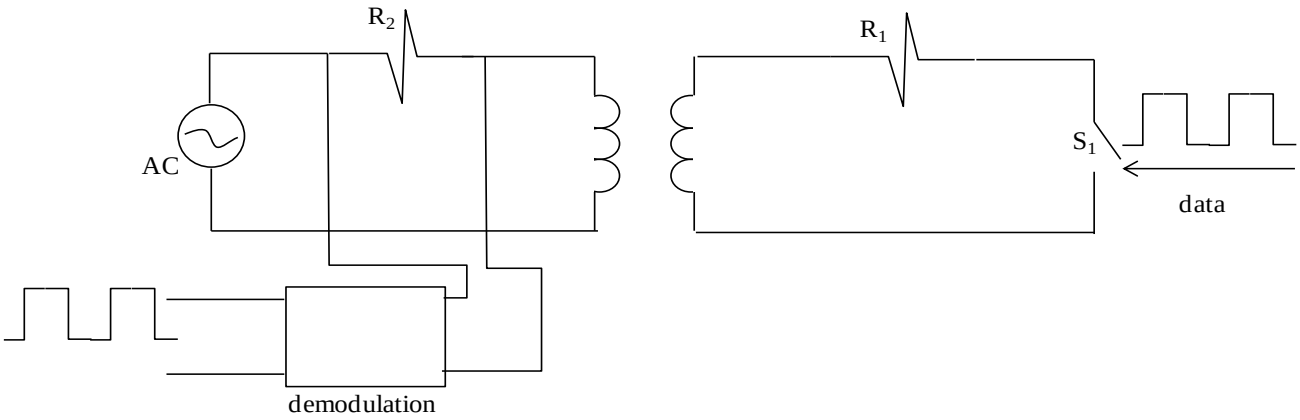

Figure 8: Signal Transmission between reader and transponder.

There is load modulation that changes the load between two stages in the transponder. While switching between two stages affects the voltage change at the reader's antenna as in Figure 6, and as the switch is alternated based on the data, the reader can retrieve the data by monitoring the voltage changes on the reader side. Due to the limitation of this technology, the reader has to be close enough to the tag to introduce inductive coupling. As the result, the typical reading distance ranges from a few millimeters up to one meter.

2.4.3 Backscattering Coupling

The efficiency with which an object reflects electromagnetic waves is described by its reflection cross-section. Thus, most antennas for active tags have a particularly large reflection cross-section for high transmission efficiency [20].

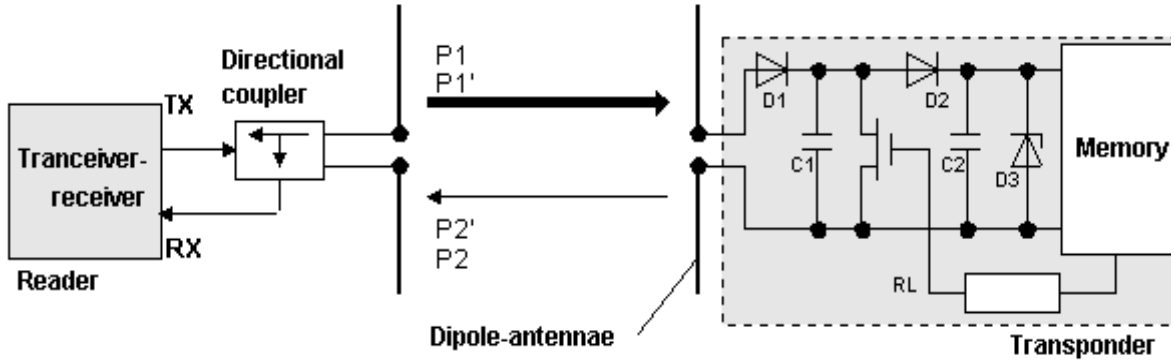

Figure 9: Operation principle of a backscatter transponder [20]

Figure 7 illustrates the data transmission process between the reader and the transponder using this technology. On the reader side, a directional coupler is attached in the front of transceiver-receiver function. Power P1 is emitted from the reader's antenna to the transponder's antenna. The power P1' is supplied to the antenna connections can be used power for the chip, while the power P2 is the reflection power of P1' by the antenna. The reflection characteristics (= reflection cross-section) of the antenna can be influenced by altering the load connected to the antenna. To transmit data, a load resistor RL connected in parallel with the antenna is switched on and off in time with the data stream to be transmitted. The amplitude of the power P2 reflected from the transponder can thus be modulated. A small proportion of P2 is picked up by the reader's antenna as P2'. This "backwards" power can be decoupled using a directional coupler and transferred to the receiver input of the reader [20].

2.4.4 Selection of the Sensing Technologies

In previous section, types of tags and different operation principles are presented. Capacitor coupling has a very limited range which is not suitable for wireless sensing requirement. Inductive coupling is generally adopted by high frequency tags and backscattering is adopted by ultra high frequency tags. Both of them have potential for wireless sensing and related literature work is presented in Chapter 3.

Based on the frequency ban, tags can be also categorized into low frequency, high frequency and ultra high frequency. Commonly, capacitor coupling is used in low frequency; high frequency tags adopt inductive coupling technique; while backscattering is employed in ultra high frequency tags. In terms of detection range, capacitor coupling is shortest while backscattering is longest. Inductive coupling is based magnetic field induce surrounded antenna which is applicable in the near field, while backscattering is based radar theory in the far field. Since the energy in the signal increases as frequency increases, the approximate reading range and data transfer rate increases when operation frequency become higher. Some characteristics of RFID are summarized in the Table 3 based on frequency range.

Table 3: RFID frequency and characteristics [19]

Ban	Low Frequency	High Frequency	Ultra High Frequency

	(LF)	(HF)	(UHF)
Frequency	30-300kHz	3-30MHz	300 MHz-3GHz
Typical RFID Frequencies	125-134kHz	13.56 MHz	433 MHz, 865 – 956 MHz, 2.45 GHz
Approximate read range	Less than 0.5 meter	Up to 1.5 meters	433 MHz = up to 100 metes 865-956 MHz = 0.5 to 5 meters
Typical data transfer rate	Less than 1 kbit/s	Approximately 25 kbit/s	433-956 MHz = 30 kbit/s 2.45 GHz = 100 kbit/s
Characteristics	Short-range, low data transfer rate, penetrates water but not metal	Higher ranges, reasonable data rate, penetrates water but not metal	Long ranges, high data transfer rate, cannot penetrate water or metals
Typical use	Animal ID Car immobilizer	Smart Labels Contract-less cards Access and security	Specialist animal tracking, logistics

Based on requirement of designing wireless sensing, a longer range of detection is preferred, and as stated in Table 3, ultra high frequency tags that adopt backscattering technique has the longest range compared to other techniques.

2.5 Choices of Antennas

A RFID system is based on the signal transmission which has both electrical and magnetic properties known as the electromagnetic wave [21]. Antenna is an important aspect of data transmission which affects range of detection and direction of electromagnetic wave propagation. There are three different types of RFID antenna structures based on the polarization directions.

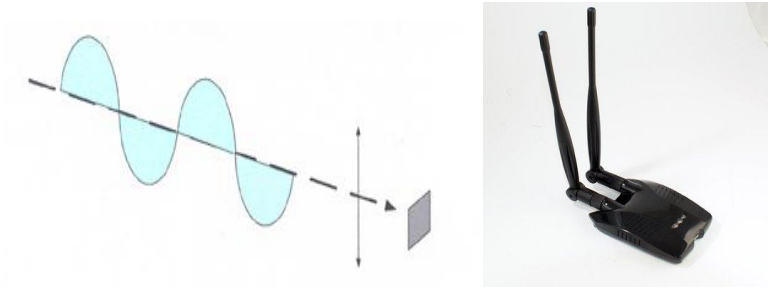

(a) (b)

Figure 10: Types of Propagation; (a) schematic of linear polarization and its direction; (b) Dual Dipole antenna[21, 22].

Single Dipole (Linear Polarization) – As stated in the words, the electromagnetic wave only propagates one direction in one plane as shown in Figure 8(a). As the propagation direction is fixed, the transmission path is fixed, so it is best for the tag orientation is known and fixed [22]. Many tags are mainly designed in this mainly due to its simple structure.

Dual Dipole – Dual dipole is an antenna with two dipoles, an implementation from single dipole. One way to create a dual dipole is connecting the end of one single dipole antenna

with the end of another one to form a "V" shape antenna with an angle between two tails as shown in Figure 8(b). This way provides the flexibility on antenna orientation as the angle between two antennas is adjustable. The dual dipole design can greatly reduce the orientation effect caused by single dipole antenna by providing two transmission paths [23]. In the RFID design, the dual dipoles usually placed orthogonally to each other achieve circular polarization.

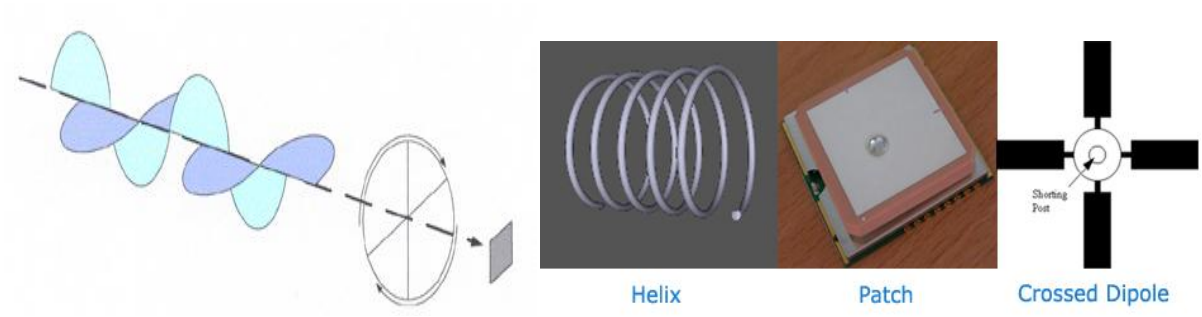

(a) (b)

Figure 11: Helix and Crossed dipoles; (a) propagation direction; (b) types of presentation: helix, patch and crossed dipole [21, 22]

Helix or Crossed dipoles (Circular Polarization) – The electromagnetic wave is capable of propagating in two planes and creating a circular effect as shown in Figure 10(a). In Figure 10(b) are some typical antenna forms which could be the structure of RFID reader antenna. Due to its continuously rotational electromagnetic field, it is able to cover any tag that is in its path, which makes it excellent detector for tags with unknown or unfixed orientations. However, comparing to the single dipole antenna, the circular polarization technique will result the loss of power at least 3dB [21]. These three types of antenna structures are commonly used in read antenna based on the application requirements.

The circular antenna can be further categorized into two families, Monostatic and Bistatic circular polarized antenna. The monostatic antenna is the common used antenna type that both the transmitter and receiver are collocated [24], meaning using the same antenna for both data transmitting and data receiving, while the transmitter and receiver are separated in bistatic antenna structure [25], meaning using separated and dedicated antennas for the transmit and receive operations. For example, a four-port monostatic reader requires four antennas; a four-port bistatic reader requires eight antennas [26]. Since both transmitting and receiving signals share the same antenna in a monostatic system, this arrangement is subject to signal reflections back into the receiver path, raising the noise floor, lowering dynamic range, and lowering reader sensitivity. However, a monostatic system is inexpensive, simple to deploy, and exhibits better data collection and processing efficiency over bistatic solutions [26].

To select the best antenna is essential in the RFID design process, and it is based on the application of the RFID. For doorway or portal tracking, a high gain antenna with circular polarization would be a good candidate, because of limited or no control at all on the items' orientations, while the RFID readers are generally fixed. The purpose of circular polarization is to provide full range detecting zone of pass by RFID tags. In order to avoid or passing through blocking substance, several circular polarized readers may be required to be installed on the two sides and top of the doorway. On the other hand, for access cards and check out station system, a low gain antenna with near filed design is enough, since the tag orientation is known and direction signal transmission can be easily established.

In terms of antenna selection, circular polarization has a better detection range but requires more energy, which can be used as the reader antenna. For the tag antenna, single dipole is most common for backscattering tags to increase the reflect directivity while circular is often applied on inductive coupling to maximize the magnetic field.

2.6 Methods of Tag Inlay

The material of the antenna is also impact and affecting the performance of data transmission as well. A lower resistively material is usually better than a high resistively. For high frequency tags, which oscillated within 13.56 MHz, any reasonably conductive metal would work, such as aluminum, copper, silver [27]. However, different materials results different specific read and write characteristics due to differences in chemical properties. A copper antenna is slightly more expensive than aluminum or silver but is more conductive and usually provides a longer distance read capability [28], such as for ultra high frequency. To compose of a chip with an antenna, technologies of inlays are involved, which should be considered in selecting tags. There are two types of RFID inlays, referred as either “dry” or “wet”.

(a) (b)

Figure 12: Types of Inlays; (a)wet Inlay;(b)dry inlay[29,30].

Dry inlay – when chip is comprised with antenna, antenna is directly attached to the substrate backing material [28] as in Figure 10(a), such as paper, PVC and PET. Usually, PVC and PET are commonly in use.

Wet inlay – it is similar as a dry inlay, but adhesive is added at the back [31], shown in Figure 10(b).

In both cases the inlay is supplied to a converter where it is inserted into a label or tag for requirement of the application [31].

Chapter 3

Review of SAW, CNT and RFID Wireless Sensing Technology

In the human history, many catastrophes have occurred, which cost tremendous loss in people's live, property and even result finance crisis, such as the earthquake, tsunami and nuclear meltdown in Japan in 2011. The tsunami alone caused more than $309 billion loss in the damage, forcing half million people away from home [32]. To reduce the impact of disasters, people started to develop monitoring and reporting systems to have better control over environment and preparation against disasters. For this purpose, many sensor technologies have been deployed to alarm the sign of changes in the environment so that an unexpected situation can be notified and possibly handled at an early stage. For example, an in-house smoke alarm is able to indicate the sign of a fire and allows people to take proper actions before the fire is out of control. When such change in the air quality is at molecular level, chemical reaction based sensing technologies, or chemical sensing technologies is used.

There are different kinds of chemical sensors, capable of measuring variety of parameters of air quality including temperature, humidity and concentration and component of the vapors. For example, D. Hauden et al [33] in early 1980s designed a SAW temperature sensor, and Jing Li et al [34] in 2003 designed a carbon nanotube sensor for gas and organic vapor detection. The initial designs of many those chemical sensors are generally wire based. However as wireless technologies grow and become mature, sensor technologies adopt the advantage of being wireless. Reindl, L.M. [35] in 2004 developed a wireless SAW temperature sensor, and in 2006 Calusdian, J. and Jing Li et al [36] implement their carbon nanotube gas sensor in [34] wirelessly. Employing wireless technologies, sensors are no longer limited by the length of the wire and gain better mobility. In addition the weight and size of the sensors are also reduced.

One major issue of being wireless is to power the sensors. An easy and common solution is to employ built-in power sources, such as batteries, as a part of sensor designs. However, as batteries have limited life cycles, periodically replacement is necessitated, while that may be neither suitable when the replacement is quite frequently and expansive nor applicable where the replacement is not acceptable, for instance, in a sealed container. Other designs generally adopt energy harvesting module to absorb certain type energy, such as piezoelectric based module for vibration and thermoelectric based module for temperature differences, and these modules generally either require directly connections to the sensors or integrated with the

sensors to power them. However, due to the limitation on the type of energy to harvest, these designs are generally energy type dependent. Researches start to look at another technology, the radio frequency (RF) after the realization of attracting energy from RF signals. The RF technology, beside of being wireless, can also be passive, meaning no built-in power sources or modules for the sensors. The entire energy that sensors consume would directly come from the RF signals received by the sensors. Thus, part of the signal energy is used to power sensors. The revolution of this technology is eliminate the concept that the power source has to be physically connected to sensors and bring the wireless technology to next level from wireless data transmission to wireless power transmission.

The work in both [35] and [36] employed the RF technologies to make the sensors "powerless". They adopted so-called radio frequency identification (RFID) tags. The RFID tag is not only wireless and passive but also is almost costless. The cost per single tag can go as low as between ¢10 and ¢20 in the large scale of production, reported by ODIN inc. in its RFID report [37]. The report also indicated the growth of demand for the RFID tag in the supply chain and other applications. One of the most notable events in driving tag demand is the adoption of the RFID technology by Walmart. Reik Read of Robert W. Baird & Company raised its 2010 estimate growth from 40% to over 125% just based on the announcement of this program [37]. Besides, it also reports Alien receives $10.9 million in new funding and announces 50% quarter over quarter growth rate over previous two quarters.

There are varies of chemical sensing technologies introduced in the past decades, widely used in gas and liquid sensing and monitoring as well as others. One major concept of gas sensing is to monitor the change of chemical properties through chemical reaction. By retrieving the change in the properties, it is able to detect the existence of certain molecular in the air or the change of the surrounding air quality. Two major technologies that adopt this technique are Surface Acoustic Wave (SAW) and carbon nanotube technologies which are reviewed hereby.

3.1 SAW Sensing Technologies

A typical SAW is composed of a piezoelectric crystal substrate with an inter-digital transducer (IDT) introduced by White RM, Voltmer FW in 1965, shown in Figure 12. Such mechanic wave only propagates at the surface of the substrate. Surface acoustic wave has existed for quite a long time after SAW is first explained in 1885. Acoustic wave is able to perform real-time measurement, with competitive pricing, high sensitivity and accuracy and intrinsic reliability [38-40].

As the energy of the SAW is confined at the surface level regardless of the thickness of the substrate, it has the potential sensitive towards any changes on the surface, such as mass loading, viscosity and conductivity. For chemical sensing, a sensitive film that responds to a specific gas is laid down on the propagation path [38-40].

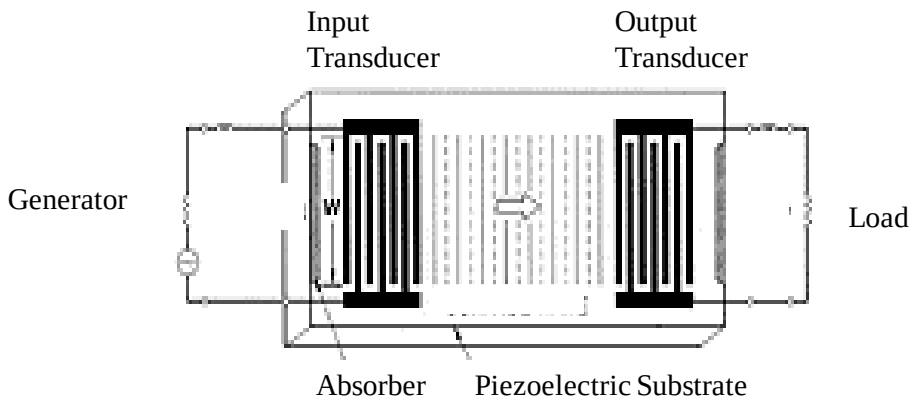

Figure 13: An example and schematic presentation of a SAW Sensor [41].

When an electronic signal is applied at the input of the IDT from one side, the measurement of the SAW is obtained at the output of the IDT on the other side. As the sensitive film reacts to the desire chemical molecular, the characteristic of the surface acoustic wave is modified due to the changes of the charges on the surface of the substrate, and such change can be measured by monitoring the target chemical molecular in the surrounding environment.

The first SAW-based sensor on solid substrate was created by Wohltjen and Dessy in 1979. The IDT was coated with a sensitive polymer layer for gas detection [42]. Since then, varies of SAW sensors were introduced to detect many physical and chemical parameters, including temperature, pressure, stress, gas flow, vapor concentration, vapor desorption and diffusivity.

In Dickert's work[43], he compared the properties of SAW resonators with QMB(quartz micro balances) for chemical sensing, which showed SAW was forty-fold higher sensitivity than QMB in detecting solvent vapors after both SAW and QMB were coated with a cross-linked β-Cyclodextrin to detect m-xylene. The author also tried molecular imprinting with both SAW and QMB. It showed that the sensor response to the vapor depended on the percentage of cross-linkers used. SAW also provides an excellent reversibility in this case. In the comparison with Thickness Shear Mode (TSM), according to Bodenhofer [44], the SAW devices is able to operate with a large amount of response signals with enhanced surface sensitivity, making it suitable for very thin layers. The SAW devices also showed advantages on the ability of multiple transduction mechanisms as a more versatile sensor platform than the TSM.

Other types of SAW sensors are also developed. In Susan's work [45], she showed the dual sensor technique with two different sensor materials was able to separate convoluted contributions between mass and modulus to the frequency response. In the experiments with A2 silica-coated quartz and Gas sensors exposed to methanol, when the methanol concentration increased, the quartz exhibited a negative frequency shifted, while Gas sensor exhibited a positive frequency shift. Shen [39] proposed a SAW sensor with coating L-glutamic acid hydrochloride which could be a good candidate for detecting ammonia gas. From his experiments, the sensitivity of the sensor was 0.10 ppm/ppm when ammonia concentration was less than 2.27 ppm. The frequency shift of the SAW sensor was 0.91 ppm, the noise level was 0.03 ppm, and the signal-to-noise ratio was 30.33. The increase of temperature would not affect the performance of the SAW gas sensors and the L-glutamic acid hydrochloride showed itself as reversible gas sensing material at room temperature. In addition, Fechete [46] presented another kind of sensor, which was consisted of layered

SAW-based gas sensors with an InOx/SiNx/36° YX LiTaO3 structure. An intermediate layer of SiNx was deposited by PECVD using SiH4/NH3/N2 chemistry at a low (<200 °C) temperature. A 100 nm InOx sensing layer was then deposited by RF magnetron sputtering. The result showed that the hydrogen adsorption into the InOx film led to an increase in its conductivity by injecting electrons into the surface, which caused a decrease in the oscillation frequency. When the SAW sensor was exposed to an oxidizing gas, the conductivity of the InOx film was decreased by removing free electrons. As a result, the oscillation frequency increased.

As demands on wireless sensing, Wen [47] introduced a RFID tag based CO2 wireless sensor by developing a SAW integrated sensor system. The ID tag and gas sensor were placed on the right side of the IDT, whereas the humidity sensor was located on the left side. The reflection peaks represented the tag's ID and data. The reading system emitted EM energy, extracting all the information from all the sensors, and recognizing environmental conditions at each sensor location through radio-frequency identification (RFID) tag. The reflection coefficient of the tag antenna was measured as well as the phase angle shifts of the reflection peaks. It showed that the phase shifts were clearly observed for different CO2 concentrations. The diversity of the SAW on gas sensing can be extended if wireless technologies such as RFID are employed as shown in Wen's work.

Table 4 presents a summary of some earlier research work done during 1981 and 1997 on SAW chemical sensors.

3.2 Carbon nanotube (CNT)

Beside SAW sensor, CNT based sensors are also received many attentions after the discovery [49, 50] of cylindrical graphene shape (shown in Figure 3) multiwall carbon nanotube (MWNT) [49] and single walled carbon nanotube (SWNT) [50] in the past two decades, which puts forwards a new technology, with high chemical and thermal stability, high elasticity, high tensile strength and metallic conductivity [49]. Since then many intense investigations and researches has been ongoing on CNT and many novel applications has occurred including scanning probes, electron field emission sources, actuators, batteries, nanotube devices [51].

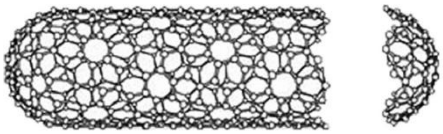

Figure 14: Structure of single walled carbon nanotubes (SWNTs) [52].

Figure 14 represents the general structure of the carbon nanotube, consisted of a cylindrical wall and two caps. However, there are research evidences showing that the purified nanotube with open-ends have a better electrochemical properties, as the dangling bonds is able to further react with chemicals[53]. Moore et al [54] reported that the ends of carbon nanotube showed excellent electrochemical properties, with reversible electrochemistry at the ends of the tubes because of the oxide species formed from the dangling bonds of carbons. Pre-treatment and purification are to improve the electrode performance, but to sense the existence of the chemical is to monitor the change in the electrode. In general, the CNT-

based gas sensing utilizes the electrical conductance change caused by the gas adsorption as the electrical readout.

Table 4: Chemicals and monitored air particles [48]

Measurand	Substrate	Chemically interactive material (CIM)
Acetone		Hydroxybutyl methyl cellulose
Methanol		Hydroxybutyl methyl cellulose
H_2	YZ-$LiNbO_3$	Palladium
	STX-SiO_2	Palladium
	Si/SiO_2/ZnO	Palladium
CH_3CHOH		Hydroxybutyl methyl cellulose
H_2O	STX-SiO_2	Phthalocyanine (PC)
H_2S	YZ-$LiNbO_3$	WO_3
	YZ-$LiNbO_3$	TEA
	YZ-$LiNbO_3$	WO_3
	RCY-quartz	WO_3
	Si/SiO_2/ZnO	WO_3
CO	STX-SiO_2	Phthalocyanine (PC)
CO_2		Phthalocyanine (PC)
CH_4	STX-SiO_2	Phthalocyanine (PC)
SO_2	YZ-$LiNbO_3$	Triethanolamine (TEA)
	STX-SiO_2	Phthalocyanine (PC)
	quartz	Heteropolysiloxane
NO_2	YZ-$LiNbO_3$	Lead phthalocyanine
	STX-SiO_2	
	YX-$LiNbO_3$	Lead phthalocyanine
	Quartz	Copper phthalocyanine
	Si/SiO_2/ZnO	Copper phthalocyanine
	$LiNbO_3$	none
NH_3	STX-SiO_2	Platinum
	RCY-quartz	WO_3
Antigen/antibody reactions	Z cut $LiNbO_3$	Biologic film
SO_2	Yz $LiNbO_3$	Triethanolamine (TEA)
Toluene	ZnO/AI/Si_xN_y	Poly(dimethylsiloxane) Ethylene/vinylacetate
CH_2CL_2		Polycarbonate resin
Humidity	STX-SiO_2	Polyethynyfluoreno
Organic vapours	ZnO/SiO_2/Si	Polymers
Vapours	ZnO/Si	Polymers

Rosen [56] applied carbon nanotubes as electrodes in gas discharge tube(GDT) in his work. The result showed that dc breakdown voltage of the GDTs was highly depended on the gas pressure and on the noble gas. However, the dc breakdown voltage of the nanotube coated GDTs decreases gradually with increasing number of surges. In general, gas discharge tubes comprising SWNT-coated electrodes had significantly improved performance in terms of dc breakdown voltage, with lower breakdown voltage and a factor of 4–20 reduction in breakdown voltage fluctuation. That could be attractive to Asymmetric Digital Subscriber Line (ADSL) and High-bit-rate Digital Subscriber Line (HDSL).

Parikh[57], in 2005, described the fabrication and performance characteristics of single walled carbon nanotube (SWNT) bundles based sensor, which was directly deposited from aqueous surfactant supported dispersions on plastic substrates. Different types of SWNT were used in sensing different vapors including NO_2, O_2, NH_3. The result evidenced the change in resistance, which was believed to be due to a work function of the tube or charge transfer interactions, and SWNT/PET also showed better electrical responses over black/PET in his work.

In the interest of carbon nanotube antenna, G. W. Hanson[55] did calculation on the properties of carbon nanotube antennas via a Hallén's-type integral equation. A carbon nanotube antenna had inherently high impedance and relatively sharp resonances with very low efficiencies compared to macro-scale antennas. However, carbon nanotube antennas were found to exhibit plasmon resonances above a sufficient frequency.

In addition, Keat [58] tested a wireless gas sensor that was comprised of a gas-responsive multiwall carbon nanotube (MWNT)—silicon dioxide (SiO2) composite layer which was deposited on a planar inductor-capacitor resonant circuit. This sensor was able to monitor carbon dioxide (CO2),oxygen (O2), and ammonia (NH3). The sensor response was reversible for O2 and CO2 but irreversible for NH3. The response time was approximately 45s, 4 min and 2 min for CO_2, O_2, NH_3. The result also showed MWNT had a lower affinity for O2 compare to CO2. The conductivity of MWNTs shifted lower when the sensor was exposed to CO2 or NH3. The MWNT was also humidity and temperature dependent.

Some of the research work is summarized in Table 5, including detection of ammonia(NH_3), nitrogen dioxide(NO_2), hydrogen (H_2) and methane (CH_4), carbon monoxide (CO), sulfur dioxide (SO_2) and hydrogen sulfide (H_2S), oxygen (O_2).

Table 5: Summary of research work on CNT-based chemical sensors [59].

Analyte	CNT Material/Method	Detection Limit
NO_2	Calculation	N/A
	bare CNTs	10 ppb
	vertically aligned CNTs	25 ppb
	metal-decorated CNTs	100 ppb
	metal oxide decorated CNTs	500 ppb
	Polymer-coated CNTs	100 ppt
NH_3	Calculation	N/A
	bare CNTs	5 ppm
	vertically aligned CNTs	5 ppm
	CNT capacitor	N/A
	CNT resonant frequency sensor	ca. 10 ppm
	metal-decorated CNTs	5 ppm
	metal oxide decorated CNTs	5 ppm
	Polymer-coated CNTs	100 ppb
	Atomically doped CNTs	ca. 1%
H_2	Pd-decorated CNTs	10 ppm
	Pt-decorated CNTs	0.4 %
	vertically aligned CNTs	100 ppm
	Cryogenically cooled CNT optical probe	4%
CH_4	Calculation	N/A
	Metal-decorated CNTs	6 ppm
CO	Calculation	N/A
	bare CNTs	100 ppm
	metal-decorated CNTs	2500 ppm
	metal oxide decorated CNTs	10 ppm
	radially deformed CNTs	N/A
	Atomically doped CNTs	N/A
	CNT capacitor	N/A
	CNT resonant frequency sensor	1500 ppm
	Polymer-coated CNTs	167 ppm
SO_2	Bare CNTs	10 ppm
H_2S	Metal Oxide decorated CNTs	50 ppm
O_2	Calculation	N/A
	Bare CNTs	N/A
	CNT SAW sensor	1500 ppm

3.3 Radio Frequency Identification (RFID) Technology

Different from above technologies, Radio Frequency Identification (RFID) is entirely wireless based. It is still a relatively new technology in chemical sensing field, evolved from identifying and tracking technology on inventory management.

A recent work [60] done by Yang et al demonstrated the great advantage of the RFID system. He revealed a three-level Zigbee RFID sensor network for inventory management applications. This connectionless tracking structure employed from RFID and Zigbee network did not require dense router, and also provided a reasonable good battery life by employing sleep mode. Originally, RFID technology serves the same purpose as bar code technology to provide unique identification of the object for easy locating and tracking. Bar codes have to be manually scanned, while RFID system can be auto controlled; Ultrasound and infrared cannot penetrate many materials, but RF signal is able to pass through many media except conductive materials and a few others; GPS, on the other hand, is not for indoor environment.

Another research done by Tseng also illustrated that ability. In this work [61], the author developed a Globally Harmonized System (GHS)-based RFID system, which was able to provide security monitoring and wireless sensing technology to collect the inventory of the chemicals, enabling the inventory control on hazardous chemicals. The usage of all the hazardous chemicals was recorded automatically, hence, ensuring the security of them. It also eliminated the human operations in the system and was able to measure the varying quantities of the chemicals in containers.

By integrating RFID technology into chemical sensing will enable the control of sensors as well as provide wireless ability to the sensors, as mentioned earlier in Wen's work [47] on surface acoustic wave. Chang synthesized a new type of antenna with an RH (relative humidity) sensing function using a modified polyimide and passive RFID. The polyimide film had on hydrophobic element and the polyimide acid is made from diamine of oxidianiline(ODA) and dianhydride of m-pyromellitic dianhydride in an aprotic solvent of N-methly-2-pyrrolidone(NMP). It operates at a humidity-dependent frequency with a sensitivity of 108kHz/%RH under 25-90%PH.

In Steinberg's recent work [62], a pH-sensitive sol–gel thin film containing the colorimetric indicator BCG was chosen as a model chemical interface with which to demonstrate the feasibility of the wireless optical chemical sensor. The optoelectronic interface of the RFID tag comprises a silicon photodiode and two light emitting diode (LED) sources measuring the optical absorption of the pH-induced color change of the thin film at two discrete wavelengths. The pH response curve and the pK value of the immobilized indicator were determined using the RFID tag system and compared with the results obtained using a standard laboratory spectrophotometer. A good correlation between the measurements was achieved, demonstrating the viable integration of an optical absorption based chemical sensor onto a passive RFID tag.

Potyrailo [63, 64] did research on RFID sensors and showed the possibility of such technology on sensing toxic vapor by directly coating the sensing film onto the RFID antenna. In his recent work, a chemical solution polystyrene sulfonate acid was coated on the surface of a RFID sensor which was then exposed to two types of toxic vapors, acetonitrile and

ethanol. The results evidenced the shifts and changes of frequencies were good indicators of the concentration of the vapors.

3.4 Summary

Based on the review in this section, Table 6 and 7 are produced as a summary of the possible candidates for sensing film and analytes as well sensing parameters that could use as the measurement and determination of the analytes.

Table 6 summarizes the sensing materials and corresponding vapors under the test. It provides a guide for sensing film selection to the target vapor. Table 7 summarizes the parameters that can be used as the indicators or the detectors corresponding to the Table 6.

Table 6: Potential sensing materials and candidates

	Chemical/Material coated	Vapors to be sensed
1	L-glutamic acid hydrochloride	ammonia gas
2	β-Cyclodextrin	m-xylene
3	A2 silica-coated quartz and Gas	methanol
4	SiNx , InOx	O3, H2
5	LiNbO3	CO2, humidity
6	SWNT/PET	NO2
7	MWNT(pyrolysis of ferrocene and xylene)-SiO2	CO2, O2, NH3
8	SnO2	CO and NO2
9	Poly file(dimethylsiloxane)	toluene
10	Polyisobutylene; polyvinyl alcohol, polyvinylpyrrolidone; polyethylene glycol, polyethyleneimine; Nafion	HCl vapor, CO2
11	Mixture of Dicyclothexylcarbodiimide(DCC) Dimethylsulfoxide(DMSO) Dichloromethane(DCM)	H2
12	-	methane, ethane, propane
13	super continuum spectrum	Carbon monoxide(CO)
14	Polystyrene sulfonate acid	EtOH, CAN, H2O
15	-	-
16	WO3	NOx, NH3

Table 7: Sensing Parameters

	Parameters				
1	Frequency and frequency shift	Concentration	Time		
2	Frequency shift due to mass loading	Resonant frequency	Layer height	Mass loading	Film layer density
3	Mass change of the methanol	Modulus change of the methanol	Frequency changes of quartz and Gas SAW		
4	Time	Frequency			
5	Antenna S11, reflection coefficient	Antenna Phase angle			
6	Voltage	Current	Time	Electric response ΔR/R	
7	Time	Relative permittivity	Conductivity	Resonant frequency	impedance
8	Current	Time			
9	Plate wave Frequency shift and frequency	Mass per unit area on the bare plate and chemical sensitive film	Wave length and optical wave length of the laser	Intensity of the laser wave	
10	Voltage	Current	Time	Electric response ΔR/R	
11	Voltage	Current	Wavelength	Transmittance	
12	Temperature	conductance	Surface Shottky barrier height, Vs		
13	Time	Wavelength	Voltage	Correlation amplitude	
14	Antenna Resonant frequency(f1 and f2)	Antenna Impedance Zp	Antenna Frequency position fp	Vapor pressure and saturated vapor pressure	
15	Antenna Resonant frequency(f1 and f2)	Antenna Impedance Zp	Antenna Frequency position fp	Vapor pressure and saturated vapor pressure	
16	Operation temperature	Annealing temperature	Vapor Concentration	Time	

Chapter 4

Theory and Modeling of Distance Effect of UHF RFID

4.1 Power and Distance

The wireless energy transmission described by Friis equation [65], with reflection coefficient [66], Γ, and polarization loss factor (PLF) [67], Γ_{PLF}, taken into consideration, is following

$$P_{Recieve} = \frac{P_{Emitter} G_{Reader}^2 G_{Tag}^2 \lambda^4}{(4\pi d)^4} |\Gamma|^2 \Gamma_{PLF} \quad (1)$$

Where,

$P_{Emitter}$	−Reader output power
$P_{Recieve}$	−Reader recieved power from tag
G_{Reader}	−Reader atnenna gain
G_{Tag}	−Tag atnenna gain
λ	−Carrier wavelength from transitter
d	−Distance between two anntenas

From Eq. (1), it shows that the received power by the tag, P_{Tag}, is inverse proportional to the second power of the distance:

$$P \propto \frac{1}{d^4} \quad (2)$$

The inverse proportionality shows that as the distance increases, the less amount of the power drops over the increment distance. Based on Eq. (2), the modeling of the received power of the tag over distance for a simple RFID system that contains one reader and one tag can be simulated as Fig. 1(a):

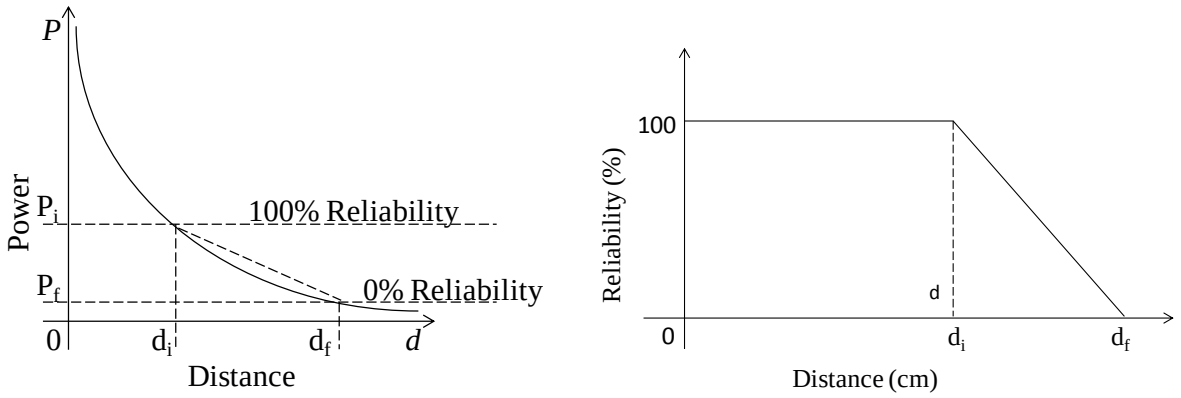

(a) (b)

Figure 15: Mapping between power and reliability of the system; (a) power levels for 100% and 0% reliability and corresponding distances; (b) linear approximation of the model and mapping from power to reliability.

When the received power is sufficient high (>P_i), the present of tag is always detected, defined as 100% reliability, while when the received power becomes insufficient to power the tag (<Pf) as the distance increases, the tag is no longer detectable, defined as 0% reliability. When the power decreases from Pi to Pf as the distance increases, the reliability is also decreasing from 100% to 0%. Thus, the percentage reliability can be mapped to the power for that range, and following equation is proposed.

$$\%\text{Reliability} = \frac{P_{Tag} - P_f}{P_i - P_f}, \text{for } P_f < P < P_i \tag{3}$$

Where,

d_i −the reading range where reliability can still remain at 100%
d_f −the distance where reliability is first reduced to 0%
d −distance between reader and tag
P_i −Tag recieved power at distance d_i
P_f −Tag recieved power at distance d_f
P_{Tag} −Tag recieved power

Thus, based on Eq. (1) and (3) the reliability in second region can be rewritten as

$$\%\text{Reliability} = \frac{d_i^4(d_f^4 - d^4)}{d^4(d_f^4 - d_i^4)}, \text{for } d_i < d < d_f \tag{4}$$

A simplified version can be obtained by applying linear approximation, presented as a straight dash line connected between 100% and 0% reliability in Fig. 1(a).

$$P_{Tag} = \left(\frac{P_i - P_f}{d_i - d_f}\right) \cdot d - \left(\frac{P_i - P_f}{d_i - d_f} \cdot d_f + P_f\right) \text{ for } P_i < P < P_f \tag{5}$$

Rearranging it, the relationship between power and distance is obtained.

$$\%\text{Reliability} = \frac{P_{Tag} - P_f}{P_i - P_f} = \frac{d_f - d}{d_f - d_i} \quad (6)$$

Based on the distances, di, df, three regions can be identified. In the first region ($d<d_i$), denoted as the stable region, the reading reliability is relatively high (100%); in the second region ($d_i<d<d_f$), denoted unstable region, the reading reliability is between 0% and 100%; and in the third region ($d>d_f$), the reliability is low and becomes zero. Depending on the range of unstable region, following two cases have been identified.

Case 1: the unstable region is quite small

In RFID design, the operation power of tag is expected to be quite low, with relative long reading distance, di, of the stable region. Thus, the unstable region, defined as df-di, is small compared to stable region. Thus, for this case, the following conditions are applied.

$$\frac{d_f}{d_i} \cong 1 \text{ and } \frac{d}{d_i} \cong 1 \quad (7)$$

Then, substitute into Eq. (4), the simplified version is given as following.

$$\%\text{Reliability} = \frac{d_f - d}{d_f - d_i} \quad (8)$$

This is the same as linear approximation of the general case in Fig. 1(b). Thus, the linear approximation could be quite accurate when the unstable region is small.

Case 2: the unstable region is large

When the d_f is getting larger, the corresponding P_f is quite small (≈0), which indicates $P_f << P_i$. Thus, Eq. (3) can be rewritten as

$$\%\text{Reliability} = \frac{P_{Tag}}{P_i}, \text{for } 0 < P < P_i \quad (9)$$

Then,

$$\%\text{Reliability} = \frac{d_i^4}{d^4} \quad (10)$$

By modeling reliability based on the distance, it is much more convenient and easier for performance prediction since distance is a parameter that is relatively easy to measure in the practical sense.

4.2 Reading period

When energy is transmitted wireless to tag, it will first charge a capacitor inside the tag to reach the operation power requirement of the tag. As the distance between tag and reader

increases, less energy is transmitted and consequently more time would be required to reach the threshold power for the tag to operate. Thus, besides increasing the output power of the reader, increasing the reading period would also extend the reading range. Other factors, such as reflection coefficient and propagation loss factor have similar effects but already included in the basic formula which is not evaluated hereby.

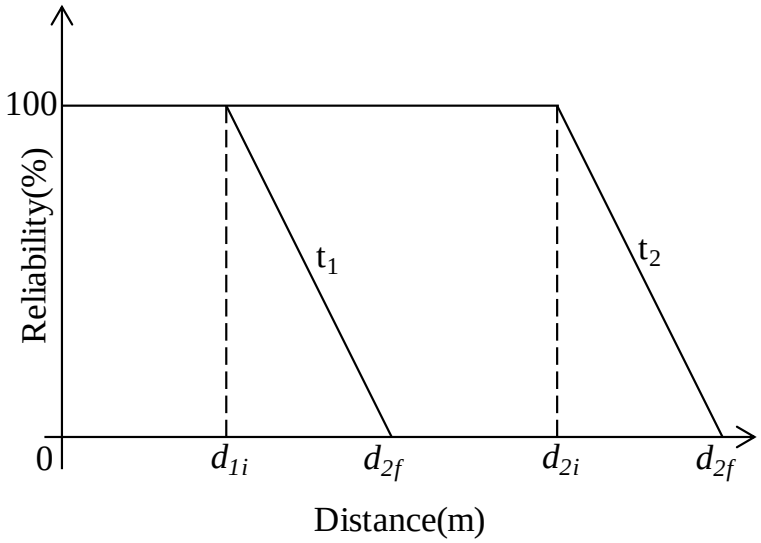

Figure 16: Illustration of two reading periods, t_1 and t_2. The maximum reading distance with 100% reliability are defined as d1i and d2i; the 0% reliability first occurs at d1f and d2f.

Figure 16 illustrates two reading periods, t_1 and t_2 respectively. d_{1i} and d1f define the unstable region for reading period t_1 while d_{2i} and d_{2f} defines unstable regions for reading period t_2. By energy equation, following equation is obtained.

$$E = \frac{1}{2}V^2C = P_{Tag\_arrive}t \tag{11}$$

Substitute Eq.(1) to Eq.(11), for different time period as illustrated in Fig. 2, the relationship between time and distance can be found for the two cases for 100% and 0% reliability respectively.

$$\frac{t_1}{d_{1i}^4} = \frac{t_2}{d_{2i}^4} \text{ and } \frac{t_1}{d_{1f}^4} = \frac{t_2}{d_{2f}^4} \tag{12}$$

Hence,

$$\frac{d_{2f}}{d_{2i}} = \frac{d_{1f}}{d_{1i}} \tag{13}$$

And,

$$\frac{d_{2f}-d_{2i}}{d_{2i}} = \frac{d_{1f}-d_{1i}}{d_{1i}} \tag{14}$$

Eq. (13) and (14) illustrate that the unstable region is proportional to the stable region for the same tag and it is independent of time.

Thus, the extended distance is following.

$$d_{2i} - d_{1i} = \left(\sqrt[4]{\frac{t_2}{t_1}} - 1\right) d_{1i} \tag{15}$$

Similarly,

$$d_{2f} - d_{1f} = \left(\sqrt[4]{\frac{t_2}{t_1}} - 1\right) d_{1f} \tag{16}$$

Combining Eq.(15) and (16),

$$d_{2f} - d_{2i} = \sqrt[4]{\frac{t_2}{t_1}} (d_{1f} - d_{1i}) \tag{17}$$

Eq. (12) and (17) shows that as time, t_2, increases, though the reading distance, d2i, would increase, the unstable region defined by d_{2f}-d_{2i} would also increase. This allows prediction of reading distance based on the time period. By performing one set measurement (t_1, d_{1f}), one is able to predict the required reading period for preferred distances. It also evidences that this is a tradeoff among reading range, power and the width of unstable region.

4.3 Reader Modeling

Many applications take the advantages of passive tags because of its relatively small size, low cost and battery-free characteristics. However, to maintain suitable reading ranges, readers are required to output more power to ensure the operation of passive tags.
Based on Eq. (1) which describes the power transmission between two antennas, the power received by the tag antenna would be:

$$P_{Tag\_arrive} = \frac{P_{Reader\_emit}\, G_{Reader}(\theta_R,\phi_R)\, A(\theta_T,\phi_T)}{4\pi r^2}$$
$$P_{Tag\_arrive} = \frac{P_{Reader\_emit}\, G_{Reader}(\theta_R,\phi_R)\, G_{Tag}(\theta_T,\phi_T)\, \lambda^2}{(4\pi r)^2} \tag{18}$$

And

$$A(\theta_T, \phi_T) = \frac{\lambda^2}{4\pi} G_{Tag}(\theta_T, \phi_T) \tag{19}$$

Where,

P_{Reader_emit} −Reader output power
P_{Tag_arrive} −Power that tag reflect back to reader
G_{Reader} −Reader atnenna gain
G_{Tag} −Tag atnenna gain
θ_R −Inclination angle at the reader
θ_T −Inclination angle at the tag

ϕ_R −Azimuth angle at the tag in the orthogonal surface
ϕ_T −Azimuth angle at the reader in the orthogonal surface
A −Effective tag antenna aperture
Λ −Carrier wavelength from transitter
R −Distance between two anntenas

In the experiments, the reader and the tag are placed face to face, light in sight, and then $\theta_R = \phi_R = \theta_T = \phi_T = 0^0$. Hence,

$$P_{Tag\_arrive} = \frac{P_{Reader\_emit}\, G_{Reader}\, G_{Tag}\lambda^2}{(4\pi r)^2} \quad (20)$$

4.4 Tag Modeling

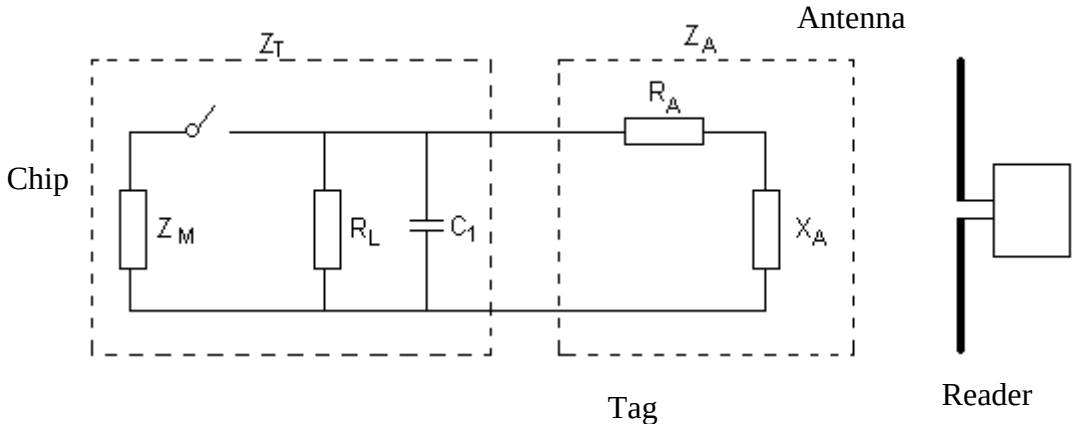

Figure 17: Equivalent circuit model of a typical tag.

Tag is another major component of RFID system, consisted of a transponder chip and an antenna, a simplified tag representation in Figure 17. Z_m is referred as modulated impedance during load modulation in backscattering process, which varies based on the stored data in the chip and generates corresponding voltage alternations on the reader side. Such voltage alternation is then demodulated to obtain the data at the reader side. R_L is referred as load resistor and C_1 is referred as charging capacitor that stores incoming energy from the reader. For maximum power transmission in the ideal case, the antenna impedance, Z_A, would match with the chip impedance, Z_T. The reflection coefficient from transmission theory provided in [64] then is calculated as following:

$$\Gamma = \frac{Z_A - Z_T}{Z_A + Z_T} \quad (21)$$

Where,
Γ −Reflection coefficient

Also, based on radar theory, the power reflected or backscattered at the tag antenna would be:

$$P_{Tag\_arrive} = \frac{P_{Reader\_emit} G_{Reader}(\theta_R, \phi_R)\sigma}{4\pi r^2} \quad (22)$$

Where,

P_{Reader_arrive} −Power that reader received from the tag

σ − Effective antenna cross section area

Then,

$$P_{Tag\_reflect} = P_{Tag\_arrive}|\Gamma|^2 \tag{23}$$

$$P_{Tag\_recieve} = P_{Tag\_arrive}(1 - |\Gamma|^2) \tag{24}$$

Where,

$P_{Tag\_reflect}$ −Power sent back to reader

$P_{Tag\_recieve}$ −Power into the tag

Substitute Eq. (6) to (3),

$$P_{Tag\_reflect} = \frac{P_{Reader\_emit} G_{Reader}\, A}{4\pi r^2}|\Gamma|^2 \tag{25}$$

That would give, assuming no other losses:

$$\sigma = A(\theta_T, \phi_T)\,|\Gamma|^2 = \frac{G_{Tag}\,\lambda^2|\Gamma|^2}{4\pi} \tag{26}$$

Based on the geometry shape of the tag, an approximation on the equation in [65] for the maximum cross section area of a rectangular flat plate is adopted:

$$\sigma_{max} = \frac{4\pi a^2 b^2}{\lambda}, \text{when } \theta_T = 0^0 \text{ and } \phi_T = 0^0 \tag{27}$$

Where

a − length of the flat plate

b − width of the flat plate

Therefore, Eq. (3) can be rewritten as:

$$P_{Reader\_recieve} = \frac{P_{Reader_{emit}} G_{Reader}^2\, G_{Tag}^2 \lambda^4}{(4\pi r)^4}|\Gamma|^2 \tag{28}$$

Chapter 5

Distance Experiment Results of UHF RFID

5.1 Experiments Setup

Experiments were conducted in an open space. Five types of Ultra-High-Frequency (UHF) metal tags and two types of ultra-high-frequency paper tags were used. One handheld RFID reader with linear polarized antenna (MC9000G, Symbol Technologies), which is similar to that used at the checkout points in glossary stores, and one fixed reader (MICRO-UHF with portable antennas, Tagsense Inc.) were used in the experiments. The output power for handheld reader is 4 watt, while the output power for the fixed reader is 50 milliwatt. Two portable antennas, 6dbi dipole antenna and 8dbi flat antenna, were used for MICRO-UHF reader.

In the range sensitivity test, the reader was fixed while the RFID tag is displaced perpendicularly to its out of plane axis (vertical position) away from the reader by incremental distances such as d1 and d2. For each incremental distance, tag presence or lack of was recorded. The maximum reading distance, df , is determined as the distance where the tag are no longer detectable and identifiable.

In the orientation sensitivity tests, tags were orientated either vertically or horizontally, at which the vertical orientation refers to the case of zero degree angle (see Figure 18(a)) and the horizontal orientation refers to $\theta=90^{o}$ (see Figure 18(b)). The range sensitivity test is repeated as the tags are placed along the horizontal orientation.

The range sensitivity tests were conducted to assess the performance of the RFID system in the presence of “obstacles” that were placed between the reader and the tag or right behind the tag (Figure 18(c)). Materials such as paper, cardboard, foam, metal and graphite composites were employed in the obstacle structures.

For above tests, there were 10 trials for each experiment which was then repeated three times or more. In this paper, data summarized in the table and figures were the average values based on 10 trials. Two criteria in the evaluation of RFID system performances were tag sensitivity and reliability.

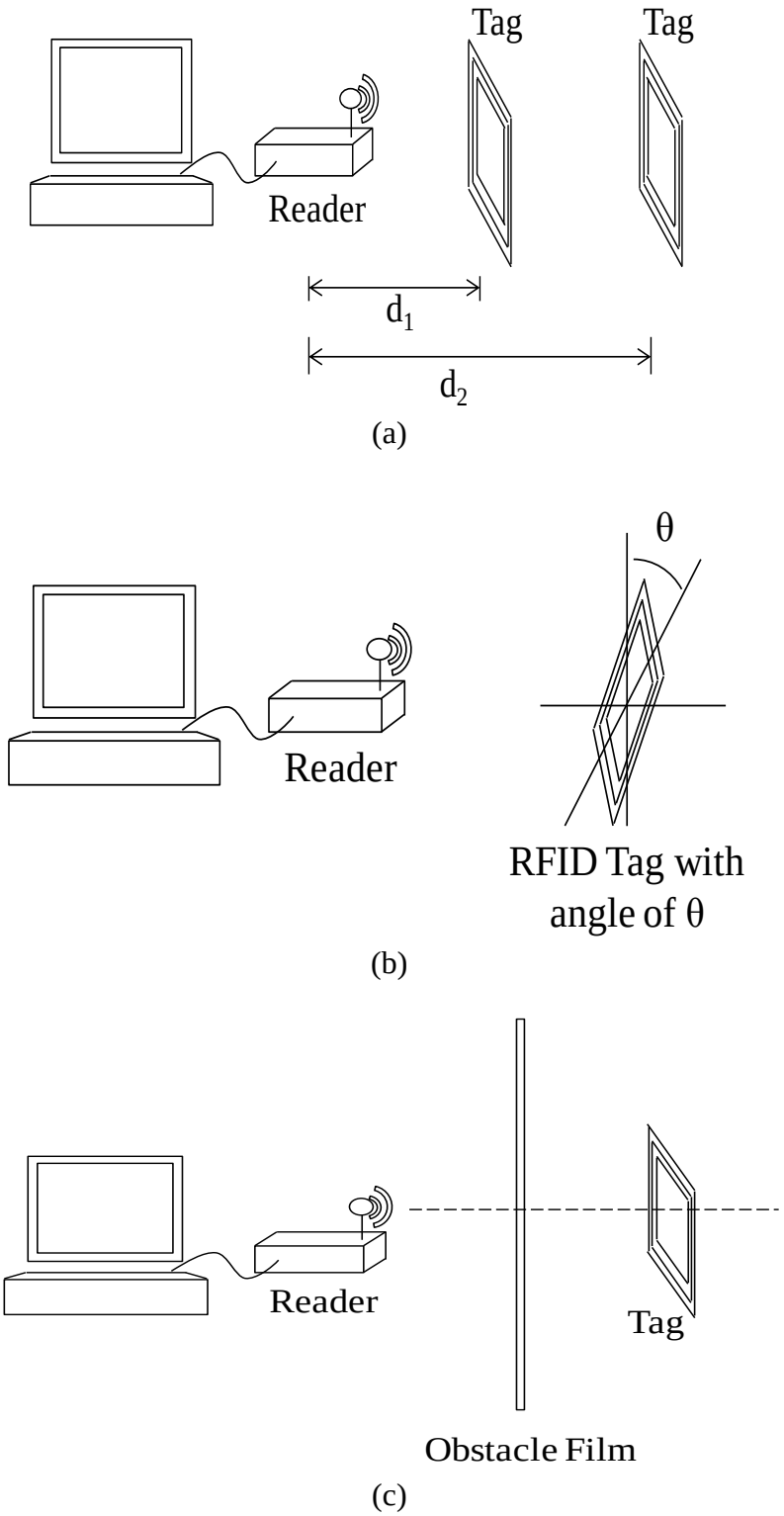

Figure 18: (a) Schematic diagram of range sensitivity with tag orientation at zero degree from the vertical plane; (b) Schematic diagram of the orientation sensitivity tests; (c) Schematic diagram of tests influencing RF signals due to obstacle film;

5.2 Range and sensitivity

It is observed that the range sensitivity spectrum can be divided into three regions. In the first region, denoted as the stable region, the reading reliability is relatively high (100%); in the second region, denoted as unstable, the reading reliability is between 0% and 100%; and in the third region, the reliability is low and eventually becomes zero. Fig. 5 illustrates these three regions for different tag orientations (vertical and horizontal). It is further noted that the presented data is the average of 10 readings conducted at 10 sec duration each. Readings at 2 sec were also conducted leading to lower reliability and sensitivity ranges, hence not reported here. In fact for the 2 sec detection response the stable sensitivity range was less than 50 cm; however, when the response time was set to 10 seconds, stable sensitivity range was doubled to 100 cm.

Table 7 shows the results for range and orientation sensitivity and reliability, using the portable RFID reader with linear polarized 6 dBi gain antenna and 915MHz UHF RFID paper tag. The processes described in Fig. 3(a) and (b) were conducted to produce this table.

Table 8: Effect of Distance and Orientation between Portable Reader and UHF Paper Tag.

Range Sensitivity d (cm)	**Tag Detection Rate (Reliability, %)**	
	Reader $\perp$ to Tag (Horizontal 90^o)	Reader $\perp$ to Tag (Vertical 0^o)
100	100	100
110	100	87
120	100	43
130	100	13
140	97	10
150	100	0
160	83	0
170	67	0
180	53	0
190	33	0
200	26	0
210	0	0

Figure 19 represents the percentage power loss in this studied region, for a horizontal tag orientation. The received power at distance 150 cm was considered as the reference power and other power was denoted as a percentage of the reference power. This power loss percentage is based on the theoretical Eq. (1) and (3), while the reliability is obtained from experimental data. The demonstration of the similarity between power and tag reliability confirmed that as the reading range increases, the reliability decreases along with the power. Above a high threshold point (the power received at a distance of 150 cm), the RFID tag can reliably be detected, below a lower threshold point (the power received at and after a distance of 200 cm), the RFID tag can't be detected at all. The measured reliability is proportional to the received power.

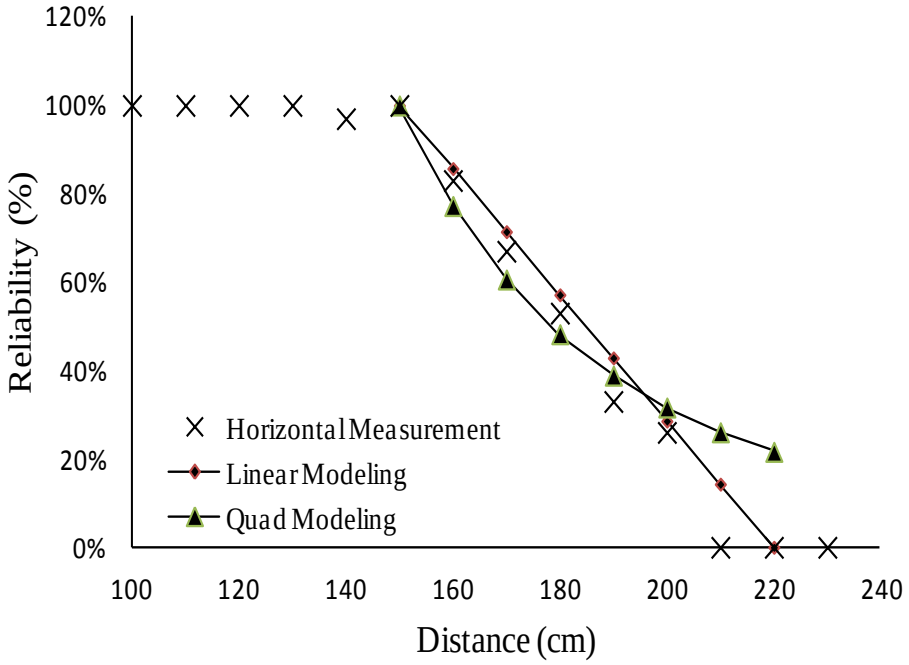

(a)

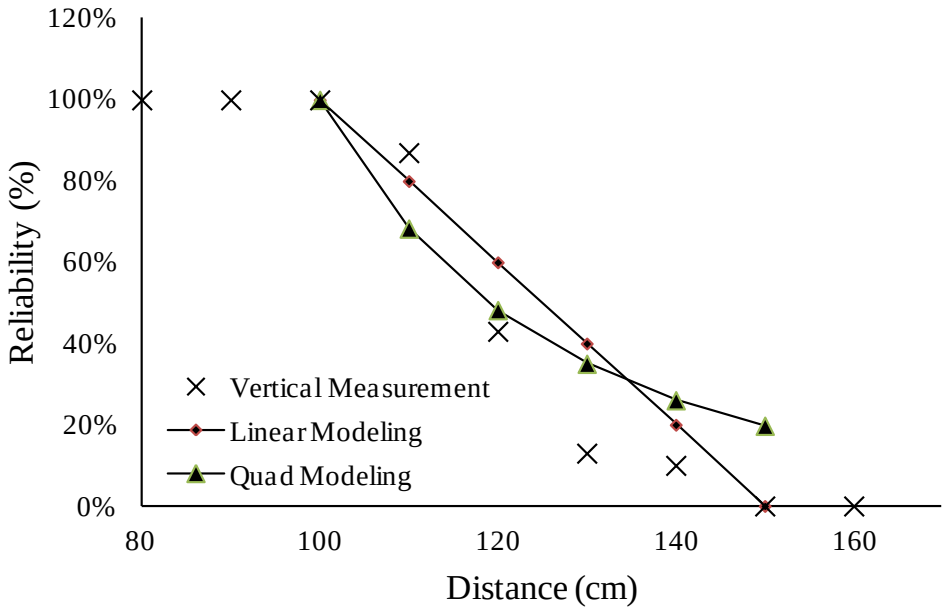

(b)

Figure 19: Reliability rate (%) drops as distance increases in the unstable region at 0^o phase shift and 90^o phase shift; (a) Horizontal measurement, 0^o; (b) Vertical Measurement, 90^o.

The prediction by the ratio is quite similar to reliability measurement. The prediction errors are approximately 7.1% for linear modeling based on Eq.(8) and 13.6% for quadratic modeling based on Eq.(10) for horizontal measurement as in Fig. 4(a). For vertical measurement, the errors are 13.9% and 15.9% for linear and quadratic modeling respectively. Linear modeling shows a better result for this tag. This also confirms that when the stable region is larger, quadratic modeling is getting more accurate, while it is opposite for linear modeling, also shown in Fig. 5. In addition, by knowing the region boundary of the transition region, the reliability of the tag in the region can be predicted directly based on the distance of the boundaries. The corresponding power can also be found based on modeling equation. Then the measurement of power loss are only required at the boundary of the transition region to obtain the full spectrum of the region.

It also notices that the measurement of the transition region is approximately 50% of the stable region for both horizontal and vertical cases. It evidences that the transition region is also proportional to the stable region by a ratio, which is also confirmed by the model and Equation (13) and (14).

5.3 Time

It is further noted that the presented data in Fig. 5 is the average of 10 readings conducted at 10 sec duration each. Readings at 2 sec were also conducted leading to lower reliability and sensitivity ranges.

Figure 20 shows the comparison between 2 second measurement and 10 second measurement. The prediction errors are approximately 11.4% for linear modeling and 28.0% for quadratic modeling in the 2 second measurement. For the 10 second measurement, the errors are 16.5% and 14.2% for linear and quadratic modeling respectively, which confirms the finding that as stable region grows quadratic modeling is more appropriate. In addition, the widths of the unstable region are 70 centimeters and 100 centimeters.

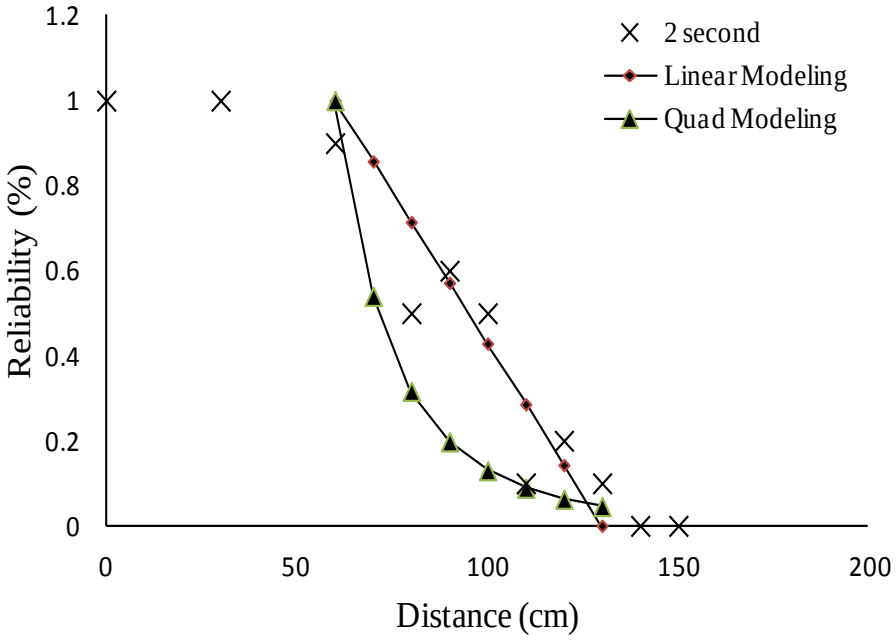

(a)

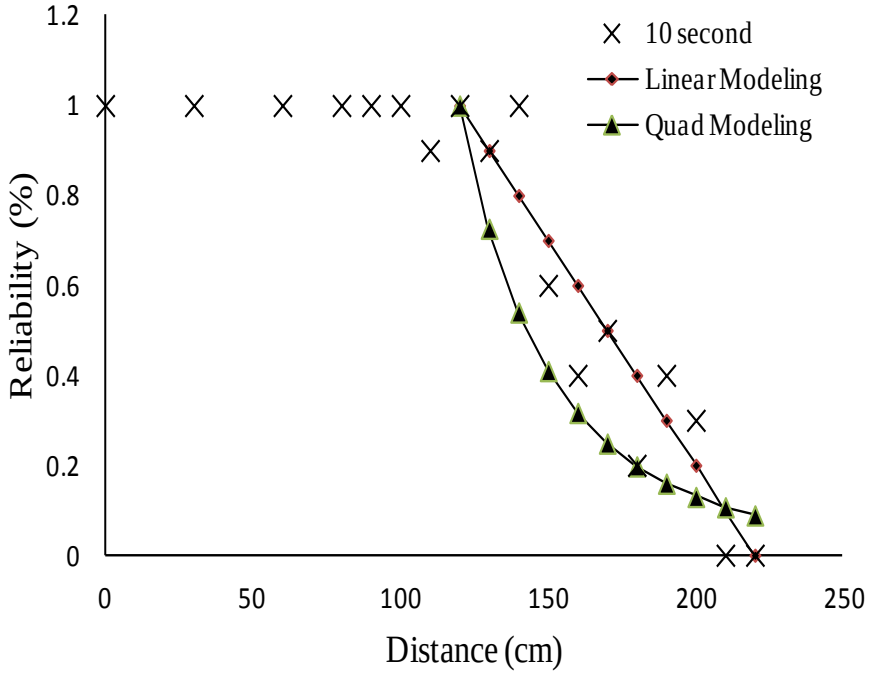

(c)

Figure 20: Measurements and experiments result for different time period which shows linear modeling has a better coherence. (a) 2 second reading period; (b) 10 second reading period.

5.4 Obstacle

In the obstacle experiment, the fixed MICRO-UHF reader, with 8 dBi gain flat patch antenna, and the 915MHz paper tag were used. A stack of paper, of different thickness was used as the obstacles. As presented in Table 8, using the flat patch antenna, the stable sensitivity range or stable region (defined as 100% reliability) was 70 cm. This is due the difference between the output powers of the two readers and the gains associated with readers' antennae.

A reliability of 100% was obtained for detection range within 12 cm for all ranges of paper thicknesses. At 100 cm, the reliability has completely degraded. It is observed that as the paper thickness increases linearly, the range sensitivity decreases exponentially. Figure 21(b) illustrates this characteristic. Additionally, as the reliability decreases, the curve shifts from left (100% reliability) to right (0% reliability). Figure 21(a) demonstrates the relationship of the percent reliability to the paper stack thickness. The solid lines represent experimental data at different distances; from top to bottom are distances 15 cm, 20 cm and 25 cm, respectively. It is observed that the reliability declined as the paper stack thickness increased; the higher the thickness, the faster the decline rate is. At a range of 20 cm, a linear relationship between the reliability and the obstacle thickness is established (dotted linear line). Such linearity provides predictive ability to assess the reliably in the presence of such obstacle.

Table 9: Effect of Obstacles between Fixed Micro-UHF Reader and UHF Paper Tag.

Sensitivity Range **d (cm)**	Tag Detection Rate **(average successful trails out of 10 trails)**			
	No obstacle	***Papers*** (15mm)	***Papers*** (35mm)	***Papers*** (65mm)
10	10	10	10	10
12	10	10	10	10
13	10	10	10	9.7
14	10	10	10	2.3
15	10	10	9.3	2
16	10	10	8.3	0
18	10	9.5	4.3	0
20	10	8.7	3.7	0
22	10	2.3	2	0
24	10	1	0	0
25	10	0	0	0
70	10	0	0	0
80	9.7	0	0	0
90	6	0	0	0
100	3	0	0	0
110	0	0	0	0

It is noted that similar trends were observed for other non-metallic obstacles; however, for metallic obstacles (e.g. aluminum alloy film), a 0% reliability was obtained for all sensitivity ranges. This was expected, since the incident electromagnetic wave was reflected by the metallic surface with a 180º phase shift [66, 67].

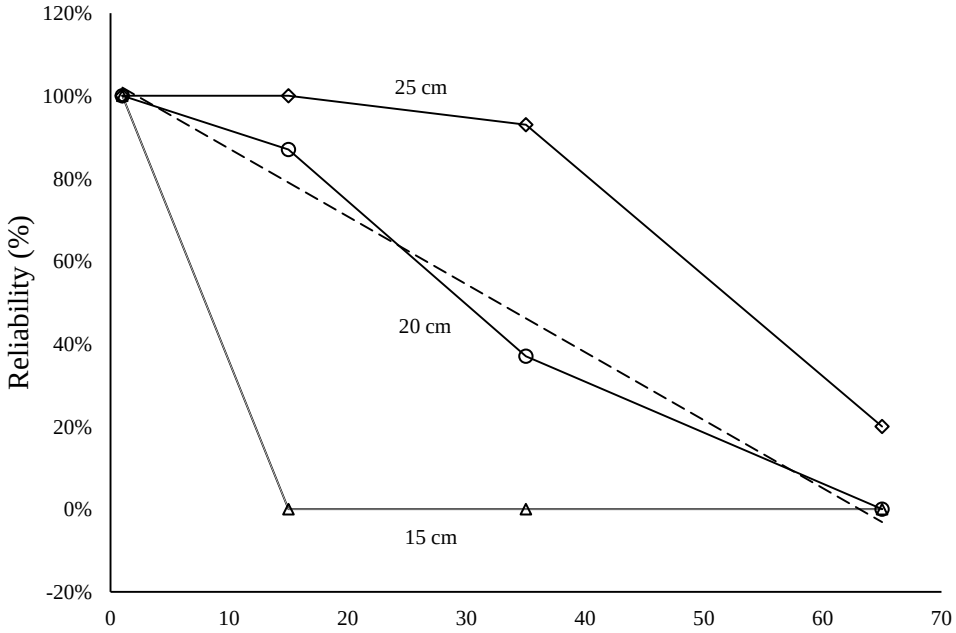

(a)

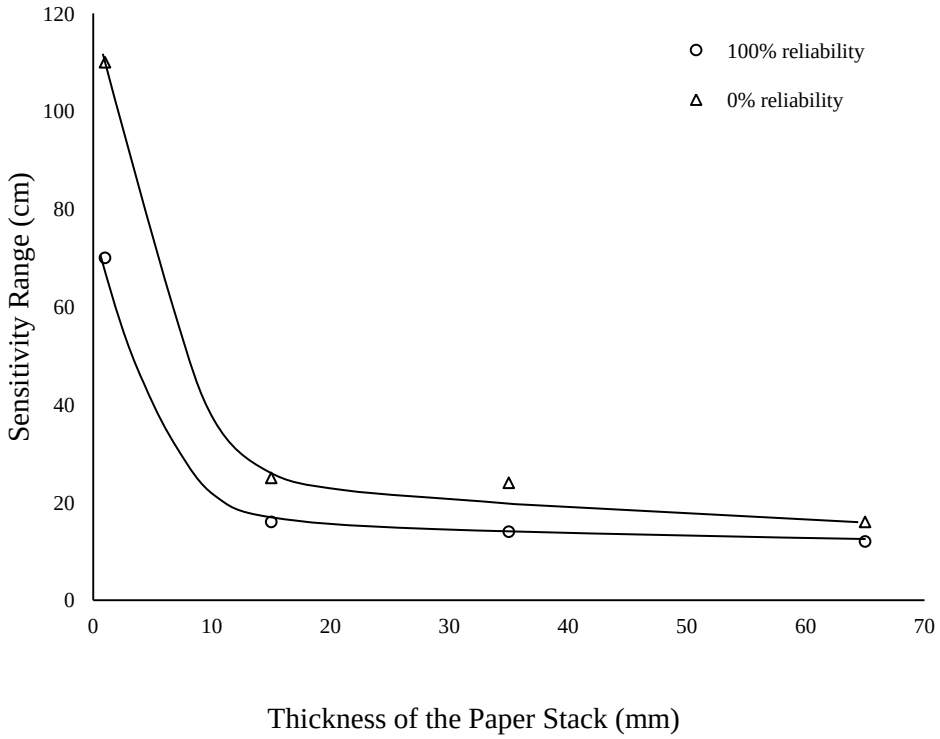

(b)

Figure 21: (a)Obstacle thickness effect on reliability; (b) Obstacle thickness effect on range sensitivity.

Chapter 6

Humidity and Temperature Experiment Result of UHF RFID

6.1 Experiments Setup

One thin (paper like) 915 MHz UHF tag (98.2 x 12.3 mm) and one 840~960 MHz flat antenna (220 x 220 x 30 mm) were used in this experimental assessment. An ESPEC (ESX-3CA) environmental chamber was used for humidity and temperature control, and an Anristu network analyzer (VNA-MS2026C) was used for data collection and analysis as in Figure 22(a). Inside the environmental chamber shown in Figure 22(b), the antenna was placed at a fixed 10 cm away from the tag. The antenna was connected to the network analyzer which was placed outside the environmental chamber. The environmental chamber's operating conditions are shown in Fig.2.

(a) (b)

Figure 22: Illustration of experimental setup; (a) environmental chamber and network analyzer; (b) tag and antenna.

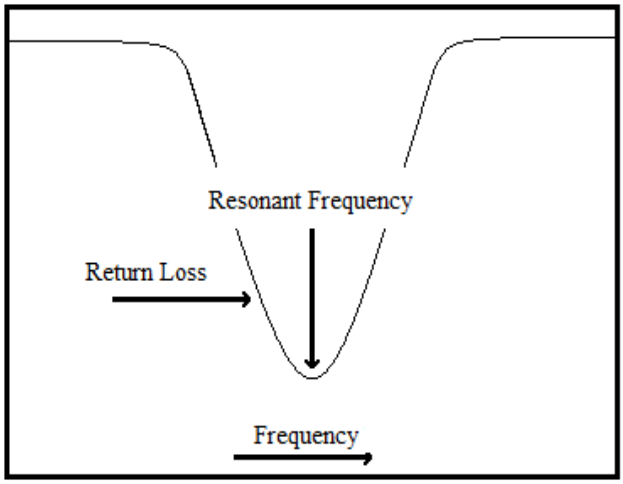

(a)

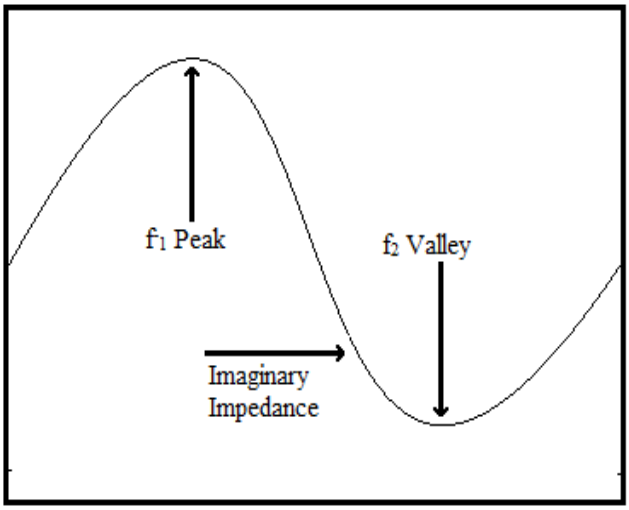

(b)

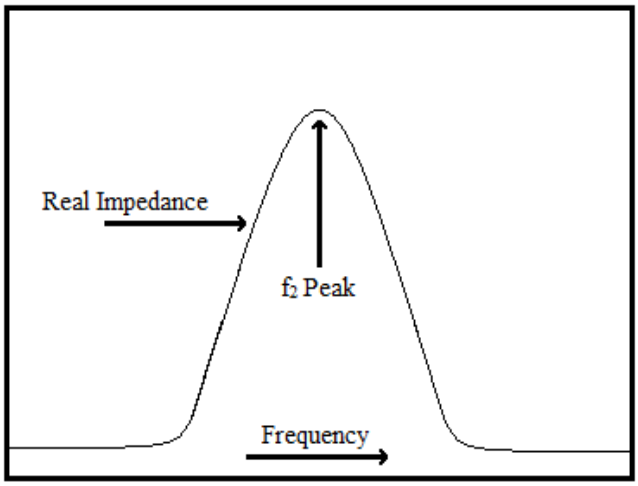

(c)

Figure 23: Frequency measurements; (a) tag's resonant frequency; (b) valley and peak frequency of the imaginary impedance measurement; (c) peak frequency of the real impedance measurement.

In this performance assessment work the tag-antenna system was subjected to a varying temperature and humidity environment. In the temperature variation experiment, the relative humidity (RH) was fixed, independently, at 50% and 80%, while the temperature increased from 20oC to 80oC at increments of 10oC. Similarly, at the same humidity levels, the temperature was ramped down at the same increments of 10oC from 80oC to 20oC. To assess the repeatability of the results the tests were repeated twice. In the humidity variation experiment, the temperature was fixed, independently, at 50oC and 80oC, while the RH varied from 20% to 80% and from 80% to 20% at increments of 10%. Similar to the temperature experiments, and to assess the repeatability of the results the tests were repeated twice.

In both humidity and temperature tests, the environmental chamber was considered as an enclosure having metal sidewalls. The adverse effects of metal on radio frequency propagation are well known and are presented in the open literature. To discern the metal effect and to project a more realistic environment, additional data was taken with the environmental chamber door open, at the above presented conditions. The door was kept open for few seconds at each test point. For example, after taking data at 50oC and 50% RH, the door of the chamber was opened, for few seconds, to allow for signal propagation and data collection for the particular condition. This process reduces the interaction of the conductive enclosure on the RF signal propagation.

In this investigation, analysis has mainly focused on the passive UHF RFID tags' resonant frequency variation as a result of environmental changes. Selected tag's frequency characteristics (Figure 23) were monitored. These characteristics include resonant frequency, imaginary impedance valley and peak frequency and real impedance peak frequency. The resonant frequency is denoted by f_o (Fig. 21(a)), the valley and peak frequencies of the imaginary impedance are denoted by F1 valley and F1 peak (Fig. 21(b)); whereas, the peak frequency of the real impedance measurement is denoted by F2 peak.

6.2 Temperature Variation Effects

In varying the temperature while holding the RH constant, a change in the resonant frequency of the RFID tag was observed, as shown in Fig. 4. In both cases where the environmental chamber door was open and closed, and at 80% RH, a linear relationship was obtained between the resonant frequency and the temperature.

In the experimental setup where the door of the environmental chamber was closed, and at 80% RH, the frequency decreased from 912.727 MHz to 909.425 MHz with a rate (slope of the trend line) of 55.05 kHz/^{o}C while the temperature increased from 20^{o}C to 80^{o}C (Figure 24(a)); when the door was open, the decrease of frequency was more pronounced and varied from 912.927 MHz to 907.524 MHz with a rate of 90.05 kHz/^{o}C (Figure 24(b)). The rate of frequency decrease is higher when the chamber door was open. This is a result of the effect of the metal enclosure on the UHF response. Although the heat transfer from the chamber to its outside, when the door was opened, might have certain effect on the frequency shift, the heat loss would result in lower temperature indicative of lesser resonant frequency shift. Additionally, the rate of decrease between the temperature ramp up and down for both closed and open chamber door, is found to be 57.1 kHz/^{o}C and 82.8 kHz/^{o}C respectively. This difference between temperature ramps up and down is believed to be due humidity variation.

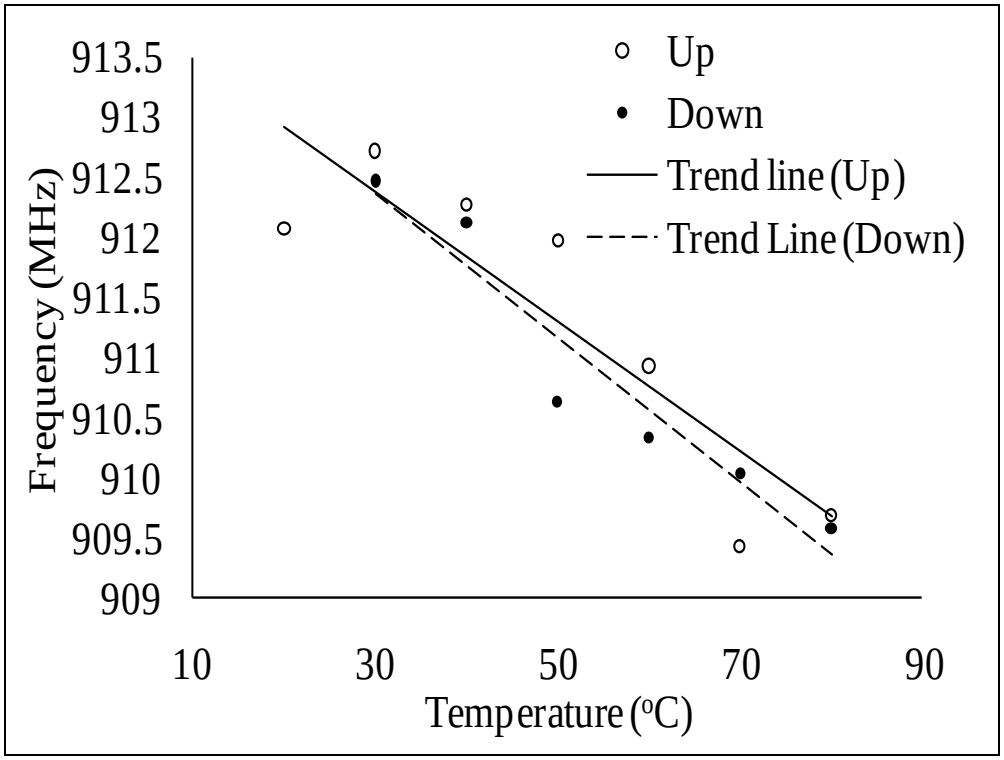

(a)

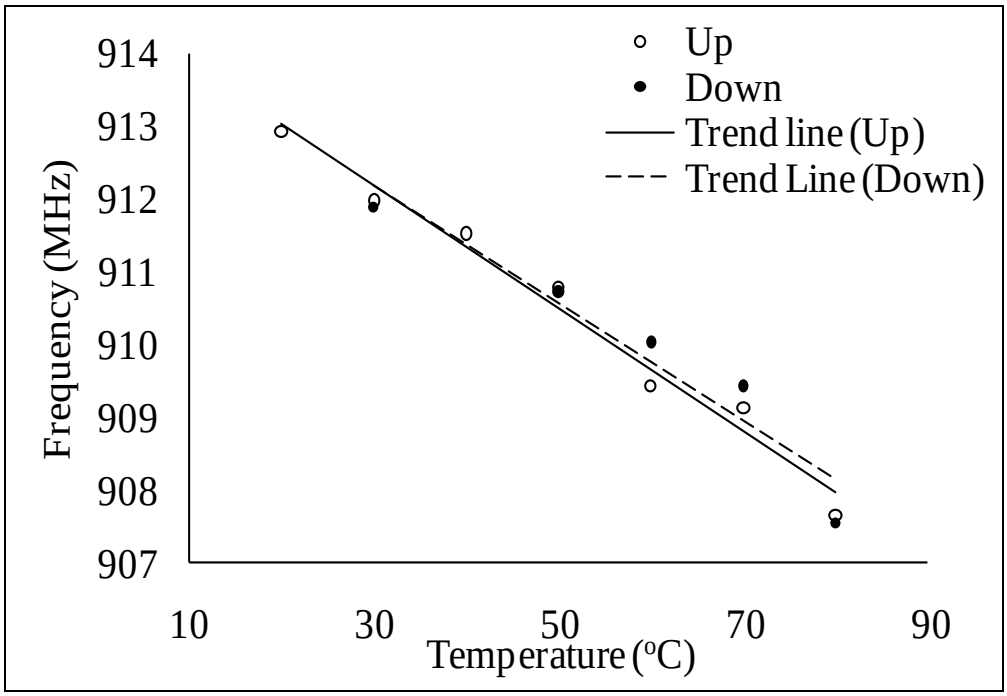

(b)

Figure 24: The resonant frequency shift as a result of temperature variation; (a) chamber door closed (at 80% RH); (b) chamber door open (at 80% RH); (c) comparison between 50% RH and 80% RH.

(c)

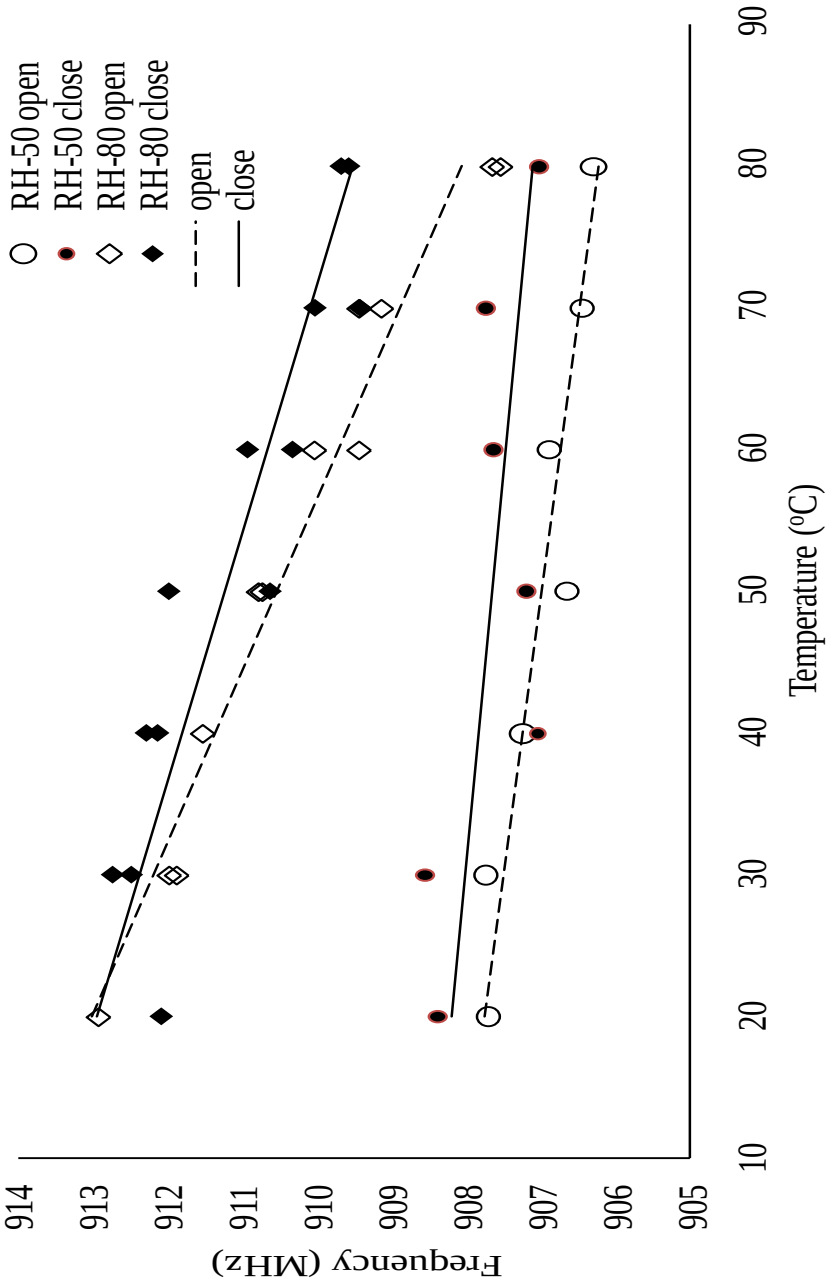

Figure 24: The resonant frequency shift as a result of temperature variation; (a) chamber door closed (at 80% RH); (b) chamber door open (at 80% RH); (c) comparison between 50% RH and 80% RH.

This difference is practically insignificant in the open door case. It is noted that the rates of increase or decrease are obtained as an averages between the ramps up and ramp down.

At 50% RH, similar frequency decreases were also observed (Figure 24(c)). A rate of decrease of 25.5 kHz/^{o}C for closed chamber door and of 25.8 kHz/^{o}C for open chamber door, were obtained, respectively. Similar to the 80% RH case, the higher rate of decrease is associated with the open door configuration, indicating the similar effects of the metallic enclosure on the RF signal propagation. Additionally, at this lower level of humidity, the rate of change was slower than at higher humidity levels. Such higher frequency variation at higher humidity level is also observed in the humidity experiment (next section). This change can be attributed to the change of antenna properties, including both resistance and capacitance. Larger variation on temperature may result higher change on the antenna resistance and capacitance, which could alter the resonant frequency further away from its nominal value.

6.3 Humidity Variation Effects

In varying the humidity while holding the temperature constant, a change in the resonant frequency of the RFID tag was observed, as shown in Fig. 5. In both cases where the environmental chamber door was open and closed, and at 80^{o}C, a linear relationship was obtained between the resonant frequency and relative humidity. In this experiment, both the humidity ramp up and down are provided at 80^{o}C but only the ramp up was recorded at 50^{o}C, unlike the case of temperature variation where both temperature ramp up and down were provided for both cases in Figure 25.

In the experimental setup where the door of the environmental chamber was closed, and at 80^{o}C, the frequency increased from 906.529MHz to 908.279MHz, for variations in humidity from 20% RH to 80%RH at intervals of 10% RH (Fig. 5(a)), with a variation rate of 12.1 kHz/RH. Whereas, in the case of open chamber door, the variation of frequency was increased from 907.126MHz to 908.627MHz (Fig. 5(a)) with a variation rate of 0.08 kHz/RH. The rate of frequency increase is higher when the chamber door was closed. This is a result of the effect of the metal enclosure on the UHF response as well as heat transfer. This difference is practically insignificant in the open door case believed to be due to reflection and deflection of water vapor at higher relative humidity level beside the metal effect caused by the chamber itself. The added reflection and deflection generally introduces phase shift to the original signal, and such phase shift can be both positive and negative, which could cause the resonant frequency shift either way. As a result, more frequency variation was observed when the chamber was closed. The gap between the two trend lines may be explained by heat transfer loss, identified earlier. The higher the humidity level, the more humidity and frequency loss would be expected when the door is open. Given the fact, the trend lines R^2 values are low for both closed and open door cases, 0.106 and 0.00001 respectively, these trend lines are not conclusive.

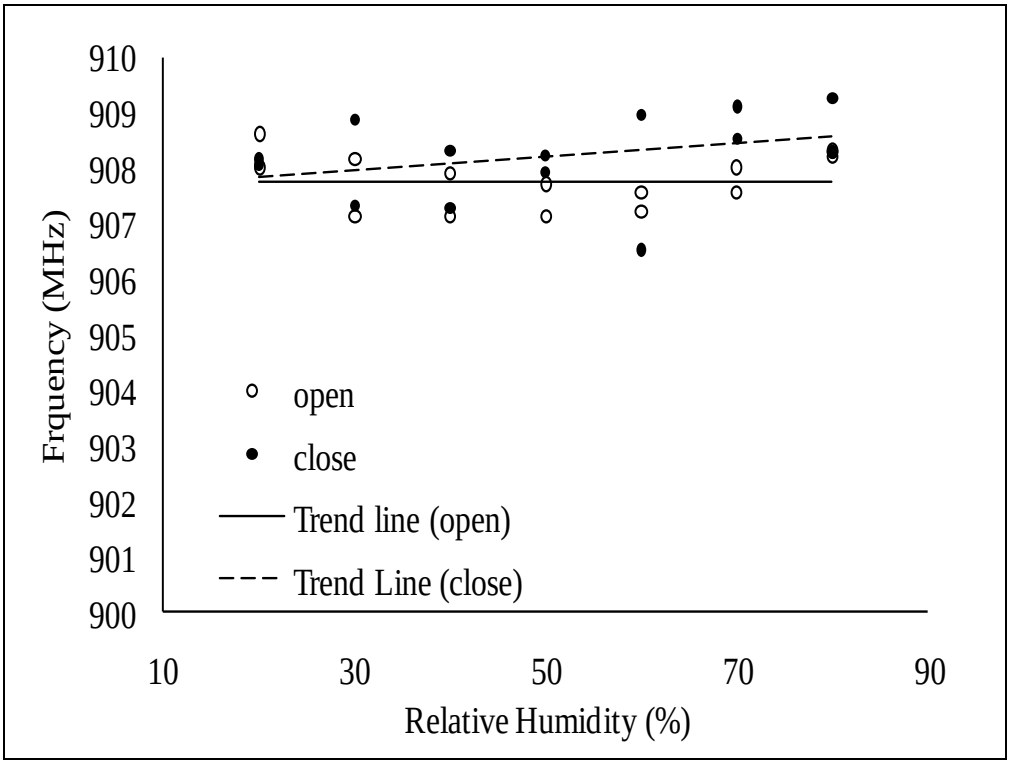

(a)

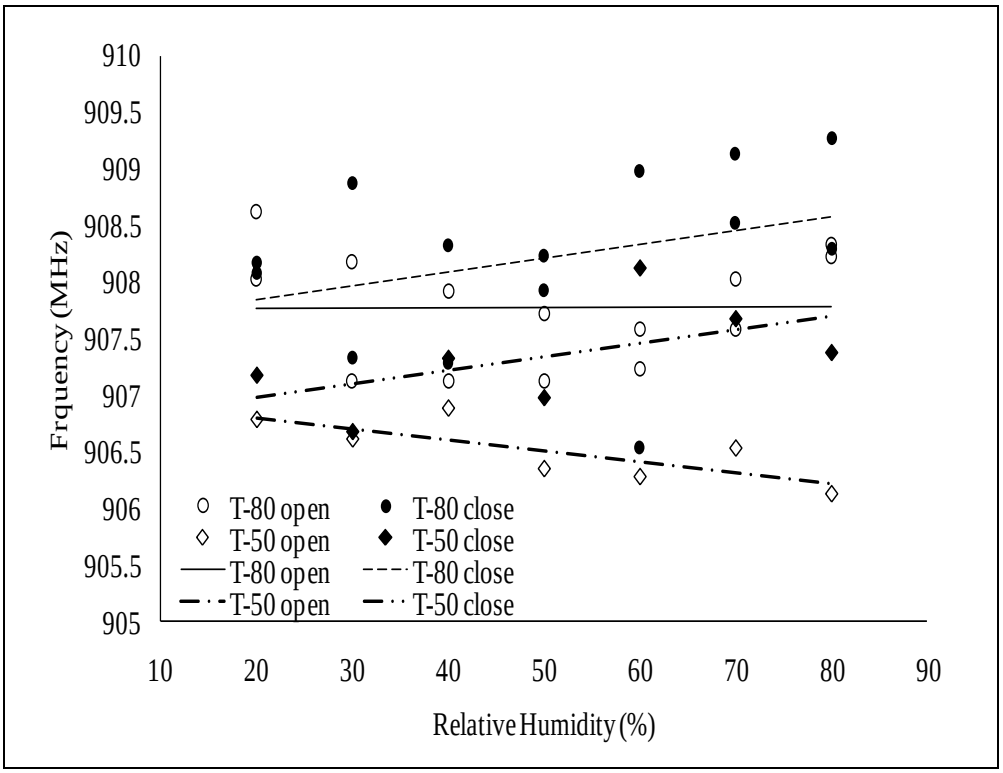

(b)

Figure 25: Resonant frequency shift due to humidity variation; (a) comparison between two cases (open and close) at 80°C; (b) comparison between 50°C and 80°C.

At 50^{o}C, similar frequency behavior was also observed in Figure 26(b). A rate of increase of 12.2 kHz/^{o}C for closed chamber door and a rate of decrease of 9.7 kHz/^{o}C for open chamber door, were obtained, respectively. Similar to the 80^{o}C, the similar rate of increase is associated with the open door configuration, indicating the similar effects of the metallic enclosure and humidity impact on the RF signal propagation and showing the repeatability of the experiment. Additionally, the constant displacement of approximately 0.88 MHz also confirmed the frequency shift due to temperature variation (previous section). Although based on Figure 26(a), the expectation of the displacement would be about 1.5 MHz, such difference could be caused by humidity variation, which is 2.75MHz. It is observed that, at both 50^{o}C and 80^{o}C, the change in frequency shift between the closed and open door configurations, increased as the humidity increased. This increase took place at similar rates but opposite direction. If the average of the frequency shift for both open and closed configurations, for both 50^{o}C and 80^{o}C, is obtained, no change of the frequency shift would be observed with increase in humidity.

In addition to the use of the UHF RFID resonant frequency, for the assessment of the impact of temperature and humidity variations on the tags response, characteristics such as impedance valley and peak frequency were also used. Figure 27 and Figure 28 present the valley frequency (F1 valley), peak frequency (F1 peak) of imaginary impedance and peak frequency (F2 peak) for real impedance at different temperature and humidity variations, respectively. These experimental conditions, for obtaining the variations in frequency, are identical to those employed in the above two sections.

Figure 27 illustrates distinctively the rate of increase of F1 valley, F1 peak and F2 peak frequencies as function of temperature increase in both, open and close door configurations and for both high and low humidity, 80% RH and 50% RH, respectively. It is observed that the rate of increase, with temperature increase was lower for open door configuration for both cases of RH. However, as seen in Fig 4.c, a higher rate of decrease was observed for the open door configuration. At this stage of the research, it is not clear why as the temperature increased the resonant frequency shifts decreased, while the F1 valley, F1 peak and F2 peak frequencies increased. The difference between the frequencies at 80% RH and 50% RH was not as pronounced in Figure 27 as was in Figure 25(c). Additionally, Figure 27 illustrates an insignificant change in F1 valley, F1 peak and F2 peak frequencies as the relative humidity increased from 20% to 80% for both open and closed door configuration and for both 80^{o}C and 50^{o}C. If the average of open and closed door configurations is taken in the case of Figure 25, similar conclusions can be drawn about the insignificance change in the resonant frequency shifts.

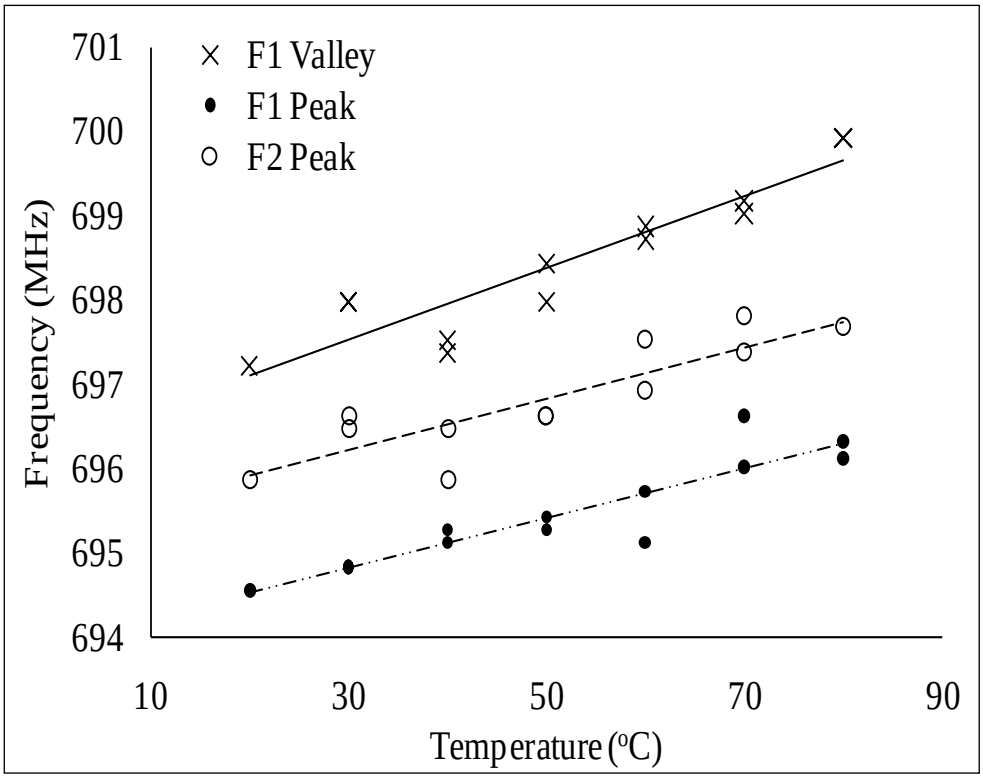

(a)

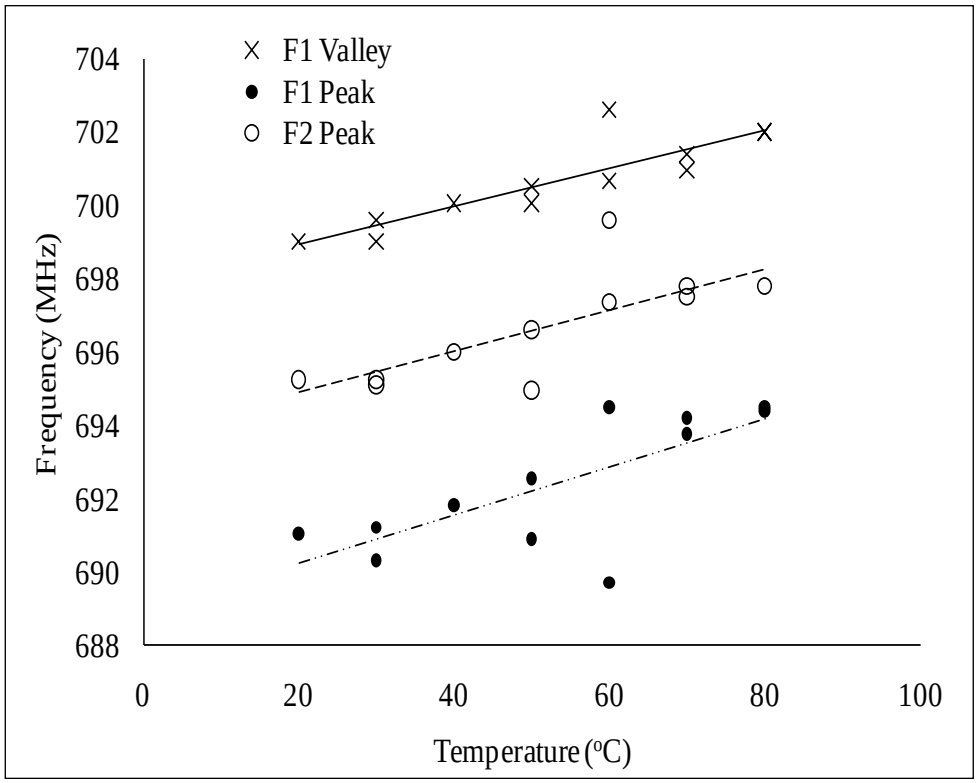

(b)

Figure 26: The peak and valley frequency shift as a result of temperature variation; (a) close case at 80% RH; (b) open case at 80% RH; (c) close case at 50% RH; (d) open case at 50% RH

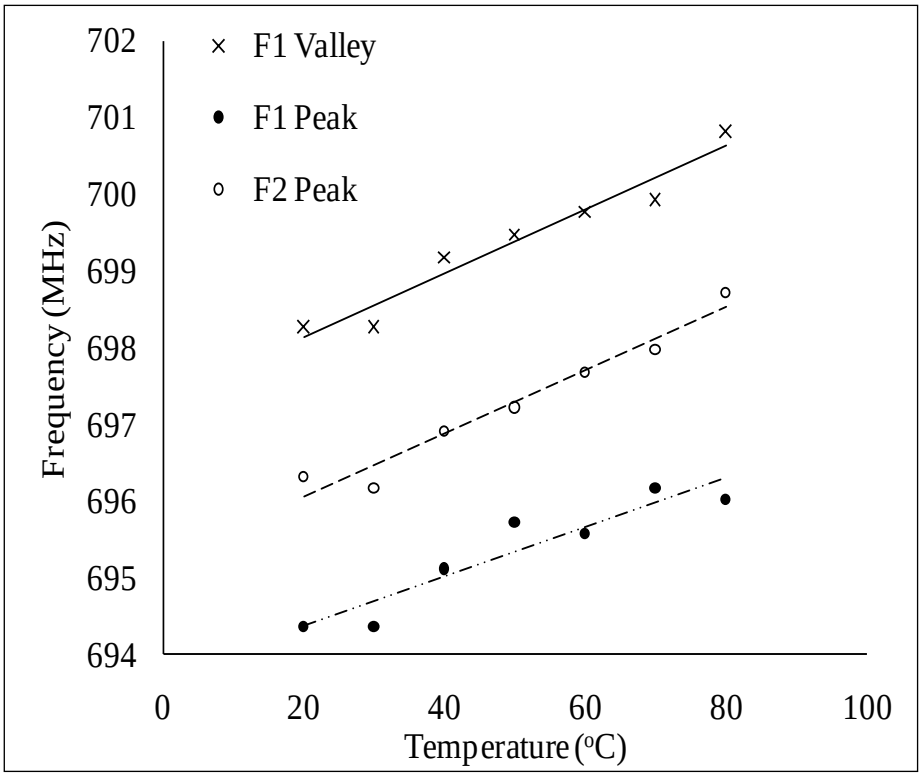

(c)

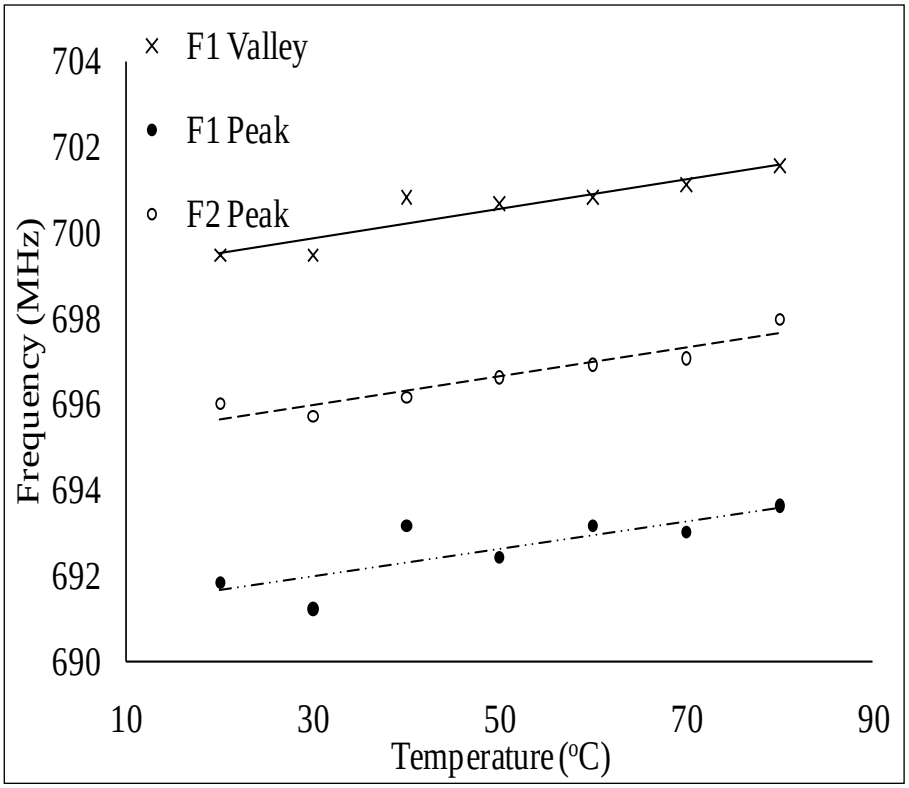

(d)

Figure 26: The peak and valley frequency shift as a result of temperature variation; (a) close case at 80% RH; (b) open case at 80% RH; (c) close case at 50% RH; (d) open case at 50% RH

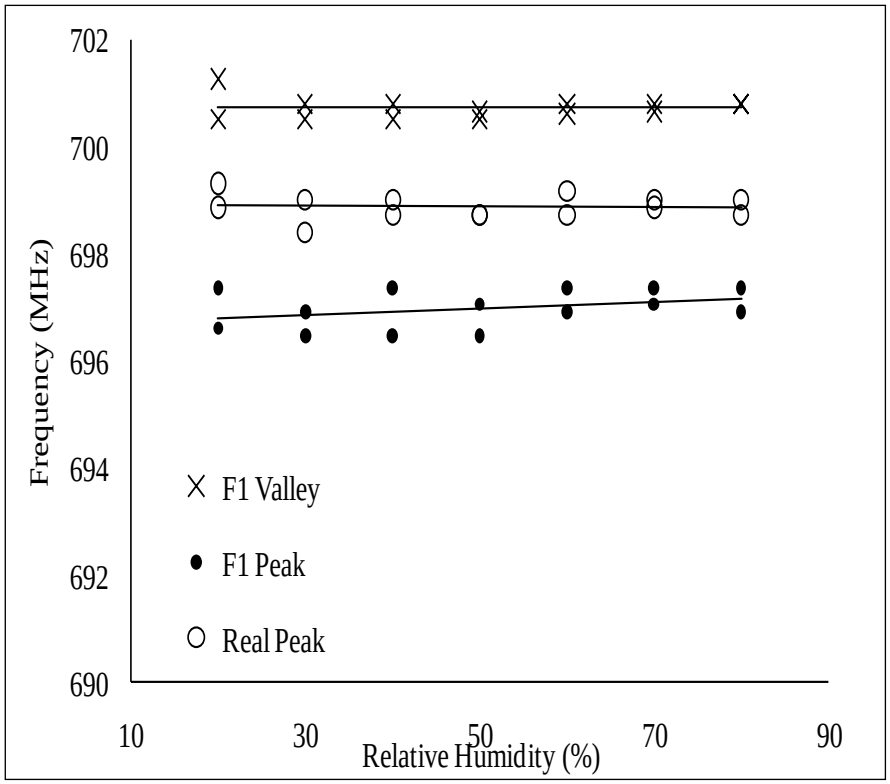

(a)

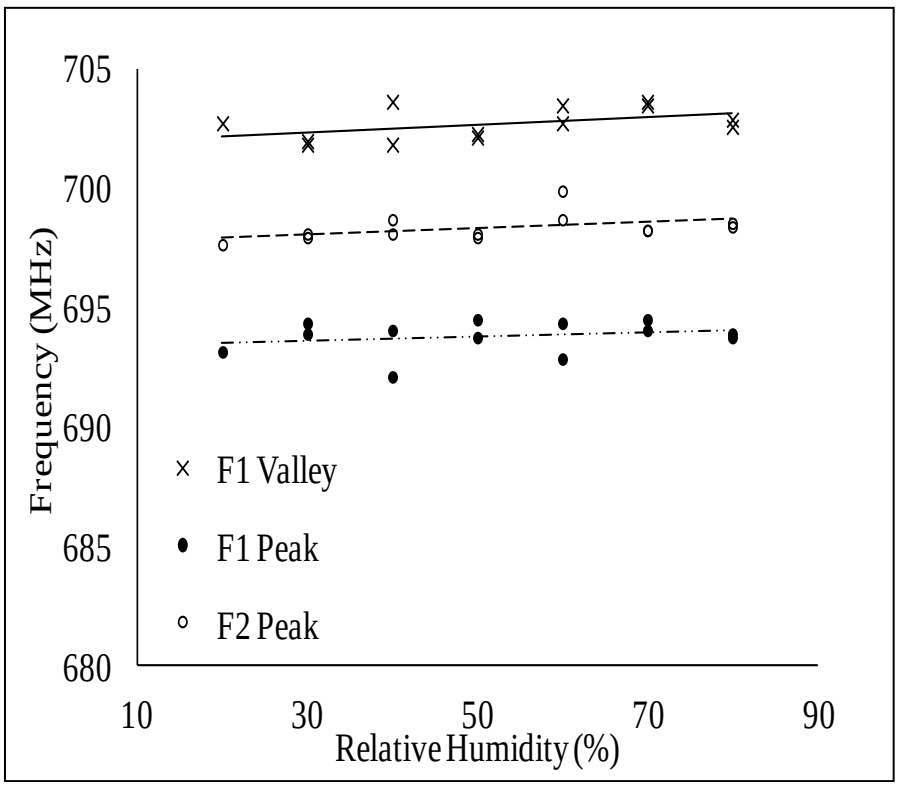

(b)

Figure 27: The impedance frequency shift as a result of humidity variation; (a) close case at 80^{o}C; (b) open case at 80^{o}C; (c) close case at 50^{o}C; (d) open case at 50^{o}C

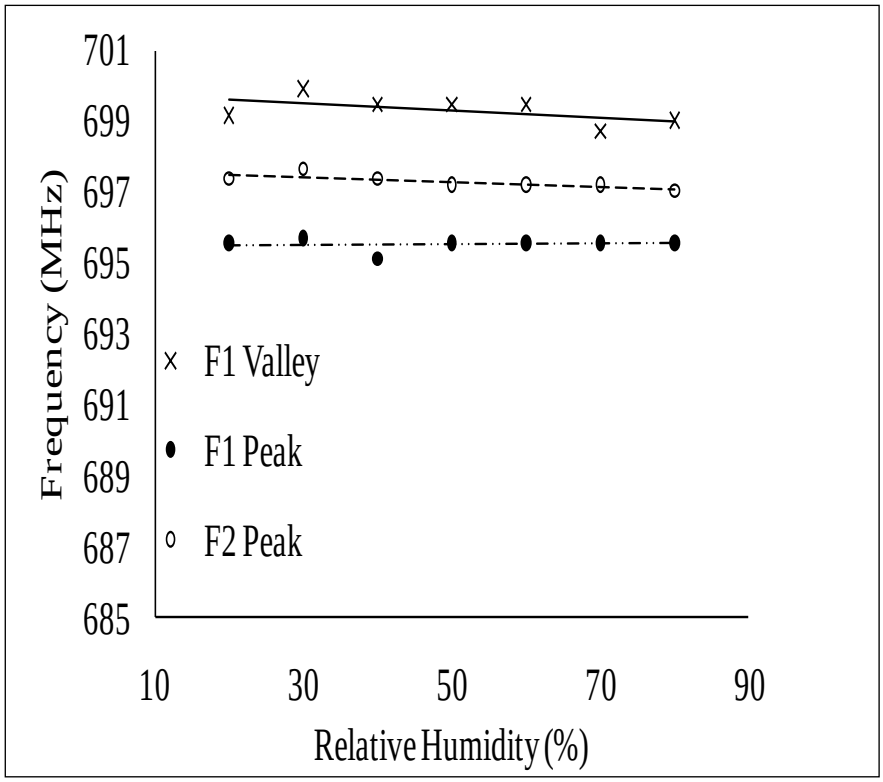

(c)

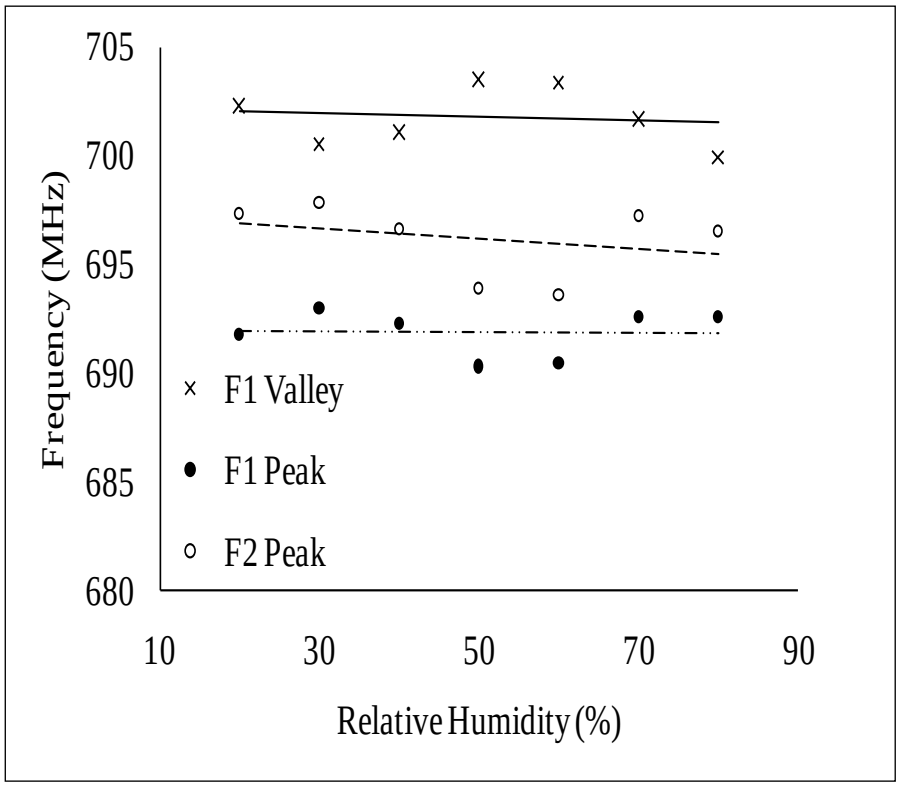

(d)

Figure 27: The impedance frequency shift as a result of humidity variation; (a) close case at 80^{o}C; (b) open case at 80^{o}C; (c) close case at 50^{o}C; (d) open case at 50^{o}C

Chapter 7

Conclusion

Our experimental studies investigate the characteristics of different tags in different environment. The tag performance data is important in tag selection for practical applications and future optimization.

The range detection sensitivity, the tag orientation sensitivity, as well as the RFID system reliability to obstacles presence have been evaluated. In the absence of obstacles, tag orientation has improved the system reliability and range of detection. Employing a higher gain antenna, the sensitivity range is improved by half of the original range, for the same reliability level. By increasing the response time, the readability increases in the unstable zone. In the presence of non-metallic obstacles, it appears the reliability and range sensitivity has not been affected by the thickness of the obstacle used. The range detection sensitivity, the tag orientation sensitivity, as well as the RFID system reliability to obstacles presence have been evaluated and matches with theoretical model. In the absence of obstacles, tag orientation has improved the system reliability and range of detection. Our experimental studies investigate the characteristics of different tags in different environment. The tag performance data is important in tag selection for practical applications and future optimization. The study on the temperatures shows that temperature has linear relationship with resonant frequency.

By knowing the region boundary distance of the transition region, the power loss in the region can be predicted directly based on the ratio of the two boundaries, and the measurement of power loss are only required at the boundary of the transition region to obtain the full spectrum of the region with 10.6% error. In addition, the linearity between time and power in the transition region can be used to predict the transition region of other reading periods by knowing one reading periods with 14% error. This could greatly simply the calculation required for three regions predictions, stable, transition and unstable regions.

An investigation on the impact of temperature and humidity variations on a passive UHF RFID system response was also conducted. UHF RFID characteristics such as resonant frequency and impedance frequency were used to assess such impact at different temperatures (20^{o}C to 80^{o}C) and relative humidity (20% to 80%) in closed and open environments.

Experimental results demonstrate a linear relationships between passive UHF RFID tags' frequency (resonant and impedance) and temperature at different level of humidity. Additionally, as the relative humidity increased, at different levels of temperature, an insignificant change in frequency (resonant and impedance) is observed, indicating the lack of influence of humidity on the tag's response. The linear relationship between frequency and temperature could be used as a temperature indicator On the other hand, for future work on the RFID tags, only temperature compensation is required. . Further investigations will focus on understanding the mechanism behind the decrease of resonant frequency and the increase of impedance frequency as function of temperature.

References

1. Peter Jones, Colin Clarke-Hill, Peter Shears, Daphne Comfort, David Hillier, Radio frequency identification in the UK: opportunities and challenges, [Online document], [Accessed 2012 Jan 24], Available HTTP: http://www.emeraldinsight.com/journals.htm?issn=0959-0552&volume=32&issue=3&articleid=857463&show=html&view=print&nolog=188313&PHPSESSID=pcctg38c1o3auuthom7ui57eq1
2. Images of RFID Tags,, [Online document] [Accessed 2012 Jan 24], Available HTTP: http://www.spychips.com/devices/tag_images.html
3. Technovelgy.com, "What is RFID?" [Online document], [Accessed on April 14, 2012], Available HTTP: http://www.technovelgy.com/ct/Technology-Article.asp?ArtNum=1
4. Mark Roberti, "Why RFID—and Why Now?" [Online document], [Accessed on April 14, 2012], Available HTTP: http://www.rfidjournal.com/article/view/7662/1
5. DataBrokers.net, "Why RFID", [Online document], [Accessed on July 15, 2010], Available HTTP: http://www.databrokers.net/why_rfid.html
6. ornl.gov, "Total Asset Visibility", [Accessed on April 14, 2012], Available HTTP: http://www.ornl.gov/sci/rf-micro/projects/totalvis.htm
7. Technovelgy.com, "RFID Reader Collision" [Online document], [Accessed on April 14, 2012], Available HTTP: http://www.technovelgy.com/ct/Technology-Article.asp?ArtNum=58
8. Technovelgy.com, "RFID Tag Collision" [Online document], [Accessed on April 14, 2012], Available HTTP: http://www.technovelgy.com/ct/Technology-Article.asp?ArtNum=57
9. Yanjun Zuo, Survivable RFID Systems: Issues, Challenges, and Techniques, July 2010, Systems, Man, and Cybernetics, Part C: Applications and Reviews, IEEE Transactions on, Volume 40, Issue 4, page: 406 – 418.
10. Corefield.com, "RFID & Public Health: A Cause For Concern?", [Accessed on April 14, 2012], Available HTTP: http://www.corerfid.com/technology/TechnologyIssues/IssuesHealth.aspx
11. Jim Wilson, "Remote Sensing Technologies and Global Markets ", February 2007, [Online document] [Accessed on April 14, 2012], Available HTTP: http://www.bccresearch.com/report/IAS022A.html,
12. Kevin Gainer, "Environmental Sensing and Monitoring Technologies: Global Markets, February 2007, [Online document] [Accessed on April 14, 2012], Available HTTP: http://www.bccresearch.com/report/IAS022A.html,
13. The electronics industry market research and knowledge network , RFID: Technology, Applications, and Global Markets, ISBN/SKU #: GB-IAS020B, and http://www.corerfid.com/Files/White%20Papers/033%20Health%20Fact%20Sheet.pdf
14. David C. Wyld, (2006),"RFID 101: the next big thing for management", Management Research News, Vol. 29, Iss: 4 pp. 154 - 173
15. Supply Chain Digest, "Understanding Differences Between Bar Code and RFID", [Online document], [Accessed on April 14, 2012], Available HTTP: http://www.scdigest.com/assets/On_Target/10-06-23-1.php?cid=3544
16. Alameed Computer Company, "RFID vs. Barcode", [Online document], [Accessed on April 14, 2012], Available HTTP: http://alameedtech.com/rfid-vs-barcode.html
17. Harland Simon Company, "RFID Tagging Technology"[Online document], [Accessed on July 15, 2010], Available HTTP: http://www.harlandsimon.co.uk/RF_Tags.php
18. UNEEDRFID.com, "How does RFID tag technology works" "[Online document], [Accessed on April 14, 2012], Available HTTP: http://www.scienceprog.com/how-does-rfid-tag-technology-works/
19. Spirit Data Capture Ltm, "RFID Technology"[Online document], [Accessed on April 30, 2012], Availble HTTP: http://www.spiritdatacapture.co.uk/rfid.asp
20. rifid-handbook.com, "Types of RFID" [Online document], Nov 14 2009, [Accessed on April 14, 2012], Available HTTP: http://www.rfid-handbook.de/rfid/types_of_rfid.html

21. SkyRFID Inc. , “RFID Reader Antenna Tutorial - What you need to know”, [Online document], [Accessed on April 14, 2012], Available HTTP: http://www.skyrfid.com/RFID_Antenna_Tutorial.php
22. Dealnay.com, “Palm Size High Power Wireless 802.11 N/G 300Mbps MIMO USB WLAN Network Adapter with 2 high gain antennas $27.95”, [Online document], [Accessed on April 14, 2012], Available HTTP: http://dealnay.com/208471/bat-palm-high-power-500mw-802.11bgn-wireless-usb-adapter-with-2-antennas.html
23. RFID Tribe, “Dual dipole antenna” , [Online document], [Accessed on April 14, 2012], Available HTTP: http://www.rfidtribe.com/index.php?option=com_content&view=article&id=169:dual-dipole-antenna&catid=27:d&Itemid=99
24. Wikipedia.org, “Monostatic radar”, Online document], [Accessed on April 14, 2012], Available HTTP: http://en.wikipedia.org/wiki/Monostatic_radar
25. Wikipedia.org, “Bistatic radar”, [Online document], [Accessed on April 14, 2012], Available HTTP: http://en.wikipedia.org/wiki/Bistatic_radar#Specific_classes_of_bistatic_radar
26. Impinj company, “About RFID”, [Online document], [Accessed on April 14, 2012], Available HTTP: http://www.impinj.com/About_RFID/About_RFID.aspx
27. BARCAMP ABIDJAN company, “HOW DO I MAKE A RFID READER ANTENNA FOR 13.56MHZ AND HOW DO I TUNE IT? WHAT WOULD BE THE BEST MATERIAL FOR IT?” [Online document], [Accessed on July 23, 2010], Available HTTP: http://www.barcampabidjan.info/how-do-i-make-a-rfid-reader-antenna-for-13-56mhz-and-how-do-i-tune-itwhat-would-be-the-best-material-for-it.html
28. AVERY DENNISON company, “RFID FAQs, What is the difference between an inlay and a label?”, [Online document], [Accessed 2010 July 23], Available HTTP: http://www.rfid.averydennison.com/faq.php
29. PCMAG.com, “RFID Inlay”, [Online document], [Accessed on April 14, 2012], Available HTTP: http://www.pcmag.com/encyclopedia_term/0,2542,t=RFID+inlay&i=56950,00.asp
30. Alibaba.com, “RFID Dry Inlay”, [Online document], [Accessed on April 14, 2012], Available HTTP: http://xingeshan.en.alibaba.com/product/328589816-209717227/RFID_dry_inlay.html?tracelog=cgsotherproduct1
31. skyRFID.com, “RFID Tag Inlays”, [Online document], [Accessed on April 14, 2012], Available HTTP: http://www.skyrfid.com/RFID_Tag_Inlays.php
32. Voice of American, Japan Tsunami Damage Cost Could Top $300 Billion, March 25, 2011, [Online document], [Accessed on April 14, 2012], Available HTTP: http://www.voanews.com/english/news/asia/east-pacific/Japan-Tsunami-Estimated-Costliest-Ever-Disaster-118644489.html
33. Hauden, D., Jaillet, G., Coquerel, R., Temperature Sensor Using SAW Delay Line, Ultrasonics Symposium, pages 148 – 151, 1981
34. Jing Li, Yijiang Lu, Qi Ye, Martin Cinke, Jie Han, and M. Meyyappan, Carbon Nanotube Sensors for Gas and Organic Vapor Detection, Nano Letters, 2003, 3 (7), pp 929–933
35. Reindl, L.M, Shrena, I.M., Wireless measurement of temperature using surface acoustic waves sensors, Ultrasonics, Ferroelectrics and Frequency Control, IEEE Transactions on, Volume: 51 Issue:11, page 1457 – 1463, Nov. 2004
36. Calusdian, J., Xiaoping Yun, Jing Li, Yijiang Lu, Meyyappan, M., Design and Testing of a Wireless Portable Carbon Nanotube-Based Chemical Sensor System, Nanotechnology, 2006. IEEE-NANO 2006. Sixth IEEE Conference on, page(s): 794 – 797, June 2006
37. ODIN inc. RFID pricing guide
38. Chi-Yen Shen, Chun-Pu Huang, Wang-Tsung Huang, “The detection properties of ammonia SAW gas sensors based on L-glutamic acid hydrochloride”, Ultrasonics, Ferroelectrics and Frequency Control, Oct. 2005, Volume 52 Issue 10, page 1877 – 1880
39. J. Hlavay and G. G. Guilbault, “Detection of ammonia in ambient air with coated piezoelectric crystal detector,” Anal. Chem.,vol. 50, pp. 1044–1046, 1978
40. C. S. I. Lai, G. L. Moody, and J. D. R. Thomas, “Piezoelectric quartz crystal detection of ammonia,” Anal. Proc., vol. 22, pp.11–13, 1985.

41. Bill Drafts, Microsensor Systems Inc, “Acoustic Wave Technology Sensors“, Oct. 1, 2000, [Online document], [Accessed on April 14, 2012], Available HTTP: http://www.sensorsmag.com/sensors/acoustic-ultrasound/acoustic-wave-technology-sensors-936
42. White RM, Voltmer FW (1965) Appl Phys Lett 7:314–316
43. F. L. Dickert, P. Forth, W. E. Bulst, G. Fischerauer, U. Knauer, “SAW and QMB for chemical sensing”, Frequency Control Symposium, 1997, Proceedings of the 1997 IEEE International, page 120 – 123
44. K.Bodenhöfer, A. Hierlemann,* G. Noetzel, U. Weimar, and W. Göpel, “Performances of Mass-Sensitive Devices for Gas Sensing: Thickness Shear Mode and Surface Acoustic Wave Transducers”, Anal. Chem., 1996, 68 (13), pp 2210–2218
45. Susan l. Hietala, Vincent M. Hietala, C. Jeffrey brinker, “Dual SAW sensor technique for determining mass and modulus changes”, Ultrasonics, Ferroelectrics and Frequency Control, IEEE Transactions on, Volume 48 Issue1, page 262 – 267
46. A.C. Fechete, W. Wlodarski, K. Kalantar-Zadeh, A.S. Holland, J. Antoszewski, S. Kaciulis, L.Pandolfi, “SAW-based gas sensors with rf sputtered InOx and PECVD SiNx films: Response to H2 and O3 gases”, Sensors and Actuators B: Chemical, Volume 118, Issues 1-2, 25 October 2006, Pages 362-367,
47. Wen Wang, “Wireless surface acoustic wave chemical sensor for simultaneous measurement of CO2 and humidity”, J. Micro/Nanolith. MEMS MOEMS, Vol. 8, 031306 (2009); doi:10.1117/1.3158610
48. C Caliendoy, P Verardiy, E Veronay, A D’Amicoz, C Di Natalez, G Saggioz, M Serafiniz, R Paolessex and S E Huqk, “Advances in SAW-based gas sensors”, Smart Mater. Struct. 6 (1997) 689–699.
49. S. Iijima, Nature 354 (1991) 56.
50. S. Iijima, T. Ichihashi, Nature 363 (1993) 603.
51. N. Li, J. Wang, M. Li, Rev. Anal. Chem. 2003, 22, 19.
52. Andrew R. Barron,, “ Carbon Nanomaterials”, [Online document], [Accessed on April 14, 2012], Available HTTP: http://cnx.org/content/m22580/latest/
    A. Koshio, M. Yudasaka, M. Zhang, S. Iijima, Nano Lett. 1 (2001) 361.
53. R.R. Moore, C.E. Banks, R.G. Compton, Anal. Chem. 76 (2004) 2677.
54. Hanson, G.W., “Fundamental transmitting properties of carbon nanotube antennas”, Antennas and Propagation, Nov. 2005, Volume : 53 , Issue:11 , page(s): 3426 – 3435
55. R. Rosen, W. Simendinger, C. Debbault, H. Shimoda, L. Fleming, B. Stoner, and O. Zhou,” Application of carbon nanotubes as electrodes in gas discharge tubes”, Appl. Phys. Lett. 76, 1668 (2000); doi:10.1063/1.126130 (3 pages)
56. Kunjal Parikh, Kyle Cattanach, Rashmi Rao, Dong-Seok Suh, Aimei Wu and Sanjeev K. Manohar , “Flexible vapour sensors using single walled carbon nanotubes”, Sensors and Actuators B: Chemical, Volume 113, Issue 1, 17 January 2006, Pages 55-63
57. Keat Ghee Ong; Kefeng Zeng; Grimes, C.A., “A wireless, passive carbon nanotube-based gas sensor”, Sensors Journal, IEEE, 2002 Apr, Volume 2 Issue 2, page 82 – 88
58. Huanjia Yang; Shuang-Hua Yang; ,“Connectionless indoor inventory tracking in Zigbee RFID sensor network”, Industrial Electronics, 2009. IECON '09. 35th Annual Conference of IEEE, 2009 Nov., page 2618 – 2623
59. Douglas R. Kauffman and Alexander Star, “Carbon Nanotube Gas and Vapor Sensors”, Angew. Chem. Int. Ed. 2008, 47, 6550 – 6570
60. Tseng, S.P.; KuoYuan Hwa; I-Fan Chang; Wenlung Li; ,“An automatic RFID and wireless sensing system on a GHS-based Hazardous Chemicals Management platform”, Embedded and Multimedia Computing, 2009, page 1 - 6
61. Ivana Murkovic Steinberg, Matthew D. Steinberg, “Radio-frequency tag with optoelectronic interface for distributed wireless chemical and biological sensor applications”, Sensors and Actuators B: Chemical, Volume 138, Issue 1, 24 April 2009, Pages 120-125
62. Radislav A. Potyrailo, "Development of radio-frequency identification sensors based on organic electronic sensing materials for selective detection of toxic vapors", J. Appl. Phys. 106, 124902 (2009); doi:10.1063/1.3247069

63. Radislav A. Potyrailo, Henri Mouquin, William G.Morris, “Position-independent chemical quantitation with passive 13.56MHz radio frequency identification(RFID) sensors”, Talanta Volume 75, Issue 3, 15 May 2008, Pages 624-628
64. Jari-Pascal Curty. Michel Declercy, Catherine Dehollain, Norbert joehl, “Design and optimization of passive UHF RFID systems”, page 43,Springer, 2007, ISBN 0-387-35274-0
65. Christophe Caloz and Tatsuo Ithoh, “Electromagnetic metamaterials: transmission line theory and microwave applications: the engineering approach” , John Wiley and Sons Inc, 2006, ISBN: 978-0-471-66985-2, Page 114
66. John S. Seybold, “Introduction to RF propagation”, John Wiley and Sons, 2005, ISBN 978-0-471-65596-1, Page 58 and Page 180
67. Christophe Caloz and Tatsuo Ithoh, “Electromagnetic metamaterials: transmission line theory and microwave applications: the engineering approach” , John Wiley and Sons Inc, 2006, ISBN: 978-0-471-66985-2, Page 114
68. J. W. CRISPIN, JR., AND A. L. MAFFETT, “Radar Cross-Section Estimation for Simple Shapes”, Proceedings of the IEEE, Volume 53 Issue:8, Aug. 1965, Page 833 – 848
69. Lingfei Mo, Hongjian Zhang, “RFID Antenna Near the Surface of Metal,” IEEE International Symposium on Microwave, Antenna, Propagation, and EMC Technologies For Wireless Communications, pp. 803–806, August 2007.
70. Leena Ukkonen, Lauri Sydänheimo, Markku Kivikoski, “Effects of Metallic Plate Size on the Performance of Microstrip Patch-Type Tag Antennas for Passive RFID,” Antennas and Wireless Propagation Letters, vol. 4, pp. 410–413, 2005.